2012

# Micro grid stability improvements by employing storage

Sumiti Lamichhane
*Louisiana State University and Agricultural and Mechanical College*

# MICRO GRID STABILITY IMPROVEMENTS BY EMPLOYING STORAGE

A Thesis

Submitted to the Graduate Faculty of the
Louisiana State University and
Agricultural and Mechanical College
in partial fulfillment of the
requirements for the degree of
Master of Science in Electrical Engineering

in

The Department of Electrical and Computer Engineering

by
Sumiti Lamichhane
B.S., Louisiana Tech University, 2009
August 2012

# ACKNOWLEDGEMENTS

First and foremost I offer my sincere gratitude to my supervisor, Dr. Shahab Mehraeen, who has supported and guided me throughout my thesis with his patience and knowledge. Without his encouragement and effort this thesis would not have been completed. I could not have wished for a better supervisor.

Special thanks also to my colleague and graduate student, Mr. Hamidreza Nazaripouya for the invaluable assistance he has provided throughout the research project. Without his knowledge and assistance, this study would not have been successful.

I am also grateful to Dr. Ernest Mendrela and Dr. Guoxiang Gu for taking time out of their schedule and agreeing to be a part of my thesis committee.

Finally, I appreciate the support and encouragement of my friends and families, particularly Shirish Lamichhane, who has always been my inspiration.

# TABLE OF CONTENTS

# LIST OF TABLES

# LIST OF FIGURES

# ABSTRACT

Storage devices can be used in a power gird to store the excess energy when the energy production is high and the demand is low and utilize the stored energy when the produced energy cannot meet the high demands of the consumers. This thesis represents a micro grid consisting of a conventional synchronous generator, as well as renewable energy sources, energy storage, and loads in order to investigate the effective energy flow control and transient stability improvement by employing thermal storage. Thermal storage, unlike electrical one (such as battery) is more environmental friendly, has longer life span, and is more effective in power flow control. In this thesis, resistive and heat pump type thermal storage are proposed and its stability effects on micro grids are evaluated. A suitable model is developed for the thermal storage and the grid's stability analysis is adopted by using linearization methods. Consequently, by designing an optimal controller for the storage the stability of the micro grid is improved as verified through the simulations.

# CHAPTER 1
# INTRODUCTION

The electricity generation, transmission, and distribution is revolutionizing due to various economic, technological, and environmental reasons. Micro grid is among the new technologies that has attracted a great attention, recently. Existing centralized grid system is actively replaced by distributed energy resources located closer to consumers to meet their requirements effectively and more reliably. Micro grid can be defined as a system or a subsystem in which the local generation is combined with the loads in a small neighborhood.

## 1.1.Micro Grid

Micro grid is a power supply network in which a cluster of small on-site generators provide power for a small community such as homes, parks, and office buildings. The increasing interest in micro grid is changing the dependency on the conventional centralized power system. In a centralized power system, power is transmitted from a large source to several utilities through a transmission line and a centralized control and hence can create shortcomings in the efficient power supply. In 1996, 12 million customers in 8 states lost power because a power line in Oregon was damaged. By contrast, by employing localized power grid or micro grid such incidents can be prevented. During disturbances, the generation and the loads of a micro grid can separate from the main distribution system to isolate the loads from the disturbance and thereby maintain the continuity and reliability of the service without harming the main transmission grid [1]. For instance, Louisiana State University (LSU) is a micro grid network connected to the main power supplied by Entergy. LSU's micro grid generates power of 20 MW using a gas turbine and distributes the power over different campus buildings. The campus gets rest of the required power from the main grid of Entergy. During Hurricane Gustav in 2008, when the rest of Baton Rouge was out of power, the buildings in LSU still had power because LSU has its own generation.

Modern micro grids are regarded [2, 3] as small power systems that confine electric energy generating facilities, from both renewable energy sources and conventional synchronous generators, and

customer loads with respect to produced electric energy. They can be connected to the main grids or operated as isolated power systems [3]. In the micro grids, alternative energy sources such as renewables can be integrated with local consumptions [3] and are more efficient and initiate less environmental issues. This, in turn, enables performance optimization and enhances the supply reliability [4]. Furthermore, since micro grids are to be on or near the site which they are to supply, losses due to transmitting electricity is relatively minimized, which makes micro-grids even more effective [5]. Finally, micro grids can be modified according to the needs of the site it will be servicing. For example, it can be used only for lighting purpose or for working on big machinery.

As discussed earlier, micro grid encourages the use of renewable energy sources. Although renewable energy resources, such as wind and solar, enhance the generation capability of a micro grid and address the environmental concerns [6], they impose economic operation and stability challenges to the micro grid due to their unpredictable nature. Power fluctuations caused by intermittent nature of the renewables should be smoothed to serve the demand more appropriately and competently. The lack of correlation between the mentioned renewable energy sources' generation trends and that of the consumption challenges the economic operation of the power grid. Some cases of the complications due to renewables are that the wind energy is mostly available during nights when the consumption is at its lowest level. Also, the peak energy from solar cells is produced in the middle of the day, which is usually not the maximum load time and no solar energy is available on cloudy days. Hence, stored energy must be utilized to compensate for calmer periods (in case of wind energy) and for the loss of sunlight (in case of solar energy).

## 1.2.Energy Storage

The use of energy storages can improve the balance between generation and demand trends, and thus, will have a significant impact on the grid's economic operation. On the other hand, the grid's dynamics and its stability rely on the amount of stored energy in the micro grid. In a conventional power system with a large number of synchronous generators as the main sources of energy, the mechanical

energy in the generators' rotors, in the form of kinetic energy, serves as the stored energy and feeds the grids in the event any drastic load changes or disturbances occur. In micro grids, energy storage will have significant stabilizing effects on the system due to the low kinetic energy stored in the micro grid's generators such as wind turbines and small synchronous generators. Consequently, the effective dynamic power flow control and stabilizing mechanisms, which engage energy storage, are of paramount importance.

Accordingly, the rising problem of imbalance between energy production and demand presented by the sporadic nature of solar and wind resources can be resolved using energy storage [7]. Storage devices can be used to store the excess energy when the production is high and the demand is low, and utilize the stored energy when the produced energy cannot meet the high demands of the consumers. Various storage technologies have emerged to fill the gap and accommodate the net demand variability [4]. The addition of storage technologies such as ultra-capacitors, conventional batteries, and heat storage can improve the economic as well as the environmental appeal of a micro grid's distributed energy resources [8]. Storage devices tend to make the net demand profile flatter and improve reliability. Among the various storage devices, the most common ones are electric and thermal energy storage.

The popular electrical storage devices are batteries and ultra-capacitors. Batteries have higher specific energy than ultra-capacitors, and thus, can provide an extra energy for a longer period of time [9, 10]. The thermal storage, on the other hand, temporarily stores the thermal energy in the form of a hot or cold medium for later use.

Electric storage has attracted much attention recently due to their technological improvements and economic advantages [11]. In most proposed micro grid operation strategies, electric storage such as batteries is used to store energy when there is extra generation, then at peak times the stored energy is instilled to the grid through power electronic inverters [12]. This will help make the generation trend flat which contributes to the use of the reserve generation capacity more economically. However, a major portion of the stored electric energy is normally converted back to thermal energy due to significant

thermal energy demand [13] and hence thermal energy storage can play an important role in meeting consumer's needs for more efficient and environmentally friendly energy use.

## 1.3.Thermal Energy Storage

An example of thermal storage is ice made during cooler and off-peak night time hours for use during the hot daylight hours. Close to 50 percent of the electric energy consumption in households, commercial, and industrial facilities are related to hot and cold water/air production in HVAC, water heater, and dryers [14]. Hence, thermal energy storage is considered one of the most important energy technologies [15]. Thermal energy storage can be used in a wide range of applications to be beneficial to the power system. The excess generation of power available during low-demand periods can be used to charge a thermal storage which increases the generation capacity during high-demand periods [15]. Thermal (hot or cold) storage devices with proper insulation can store the energy for a reasonable period of time and reduce the need for the electric storage which are the sources of harmonic distortions due to power electronics, which can be significant in micro grids with higher power ratio from the renewables to the conventional synchronous generators [16].The consumers with the thermal energy storage can shift their energy purchases to the low cost periods (off peak hours), thus saving themselves some money and putting less stress on the grid during peak hours.

Finally, thermal storage can be used to reduce the usage of batteries to decrease the amount of chemical disposals. Also, thermal storage has longer life (17 years) compared to batteries (5 years) [17]. Therefore, using thermal storage is more economic and environmental friendly [15]. Table 1.1 indicates the comparison between battery and thermal storage based on their energy parameters [17].

Table 1.1 Comparison of energy storage devices

| Description | Battery | Thermal |
|---|---|---|
| Maximum absorbed power (KW) to the maximum capacity (KWH) | 0.1 | 0.25 |
| Maximum discharged power (KW) to the maximum capacity (KWH) | 0.25 | 0.25 |

## 1.4.Objective of the Thesis

The thesis objective is to design a controller for the storage and use it as the major energy storage in a micro grid and demonstrate that the micro grid's stability can be greatly improved by the use of storages. Thermal energy storage has been tested in various applications [13] already, but the focus of this thesis is on the potential of energy storage to provide effective energy flow control, stabilizing mechanism, and demand response. Storage devices can provide the instantaneous active power required to support the dynamic stability of micro grid by varying the rate of absorbed power. In this thesis, the performance of thermal storage is also compared to that of a power system stabilizer (PSS) and governor of generator and battery to prove the superiority of the former. The following contributions are proposed to substantiate that by employing storage performance of micro grids is improved over conventional PSS and governor:

1) Dynamic behavior of micro grid components is shown to be improved and stability is recuperated faster by storage.
2) Storage's performance is robust against the sudden change of load which is desired for a micro grid network.
3) Storage provides a flatter energy generation trend despite the intermittent nature of the renewable resources.

## 1.5.Approach of the Thesis

The thesis objective will be achieved by simulations using the micro grid dynamic model. Firstly, a micro grid model is developed comprising of a generator, distributed generations, loads, and thermal storage followed by model simplification. Then, different scenarios such as a three-phase fault, sudden load change, and intermittent nature of the renewables are planned in the complete model to study the response of the generator and the model under these circumstances. Finally, an optimal controller is designed and the simulations are performed in MATLAB/Simulink environment to show that the micro

grid's stability and demand response is significantly improved when the storage (controller) is utilized compared to conventional stabilizers such as governor and PSS.

The designs will be implemented on two different topologies in simulation environments. The first demonstration will be a micro grid model with a synchronous generator, one transformer, renewable sources of energy, and constant and variable loads. Next, a different simulation is performed on a larger micro grid based on LSU micro grid topology. Both simulations will demonstrate that by applying storage, a better stability for the micro grid is obtained over the conventional power system stabilizer and steam governor. Also, due to thermal storage's more durability, higher power rates, and better environmental impacts, it is a convenient method to be used in the grids to improve demand response [18].

In order to achieve these goals, first, a proper micro grid nonlinear model is developed to include the thermal storage. Linearization method is then applied to convert the micro grid nonlinear model to a linear one. Next, an optimal storage power controller is designed, using the micro grid linearized model and LQR optimal controller, and applied to the system. Then, simulations are performed for a variety of cases and the results are recorded, compared, and studied.

This thesis is organized as follows. First, micro grid model development, as well as power system stabilizer, governor, renewable energy sources, and the thermal storage models are introduced in the next chapter. The stabilizing storage controller design is introduced in chapter 3. Next, the theoretical conjectures are verified through simulation results in chapter 4. Finally, all the deductions are concluded in chapter 5.

# CHAPTER 2
# MICRO GRID MODELING AND THERMAL STORAGE

This chapter gives an insight to the modeling and design of the several entities of this thesis. The objective of this chapter is to discuss the modeling including the equations involved of synchronous generators (with exciter, power system stabilizer, and governor), thermal storage, renewable sources, and power balance equations that make up the power system of the micro grid.

Recently, micro grids have earned numerous research interests because they can provide high quality, uninterrupted power supply to the consumers. Micro grids that are connected to the grid or independent are feasible and highly beneficial. Figure 2.1 shows the micro grid seen together with the main transmission grid [5]. Currently several research groups around the world are investigating the feasibility and benefits that micro grids may provide. There might be some issues related to micro girds such as harmonics associated with the system, however this thesis does not attend such problems, but concentrates only on modeling of the system for the investigation at various conditions such as fault and sudden load change.

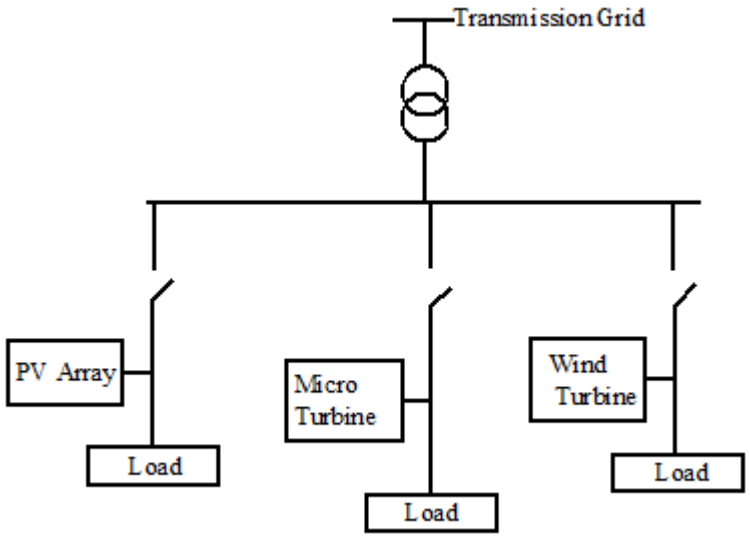


Figure 2.1 A micro gird structure seen together with the transmission grid

The first micro grid under study in this thesis is an isolated system as depicted in Figure 2.2 and is comprised of a conventional synchronous generator powered by a steam turbine, constant and variable loads, energy storage, and renewable sources of energy (wind and solar) which are connected to the grid via power electronics and transformers. The second micro grid in this thesis is connected to the main grid and like the first model is comprised of a steam turbine, loads, storage, and distributed generation. In both the cases, the synchronous generator is equipped with exciter, power system stabilizer (PSS), and steam governor. The renewable sources operate at maximum available power (from wind or solar) to save costs of extra control mechanisms such as pitch control as well as to exploit the maximum natural energy. Thus, their power is subject to change as the ambient energy fluctuates. Micro grid can be represented by a set of differential and algebraic equations to be solved simultaneously where the differential equations represent the synchronous generator dynamics and the algebraic equations describes the power balance in the micro grid. In the rest of this section we model various equipment of the proposed micro grid.

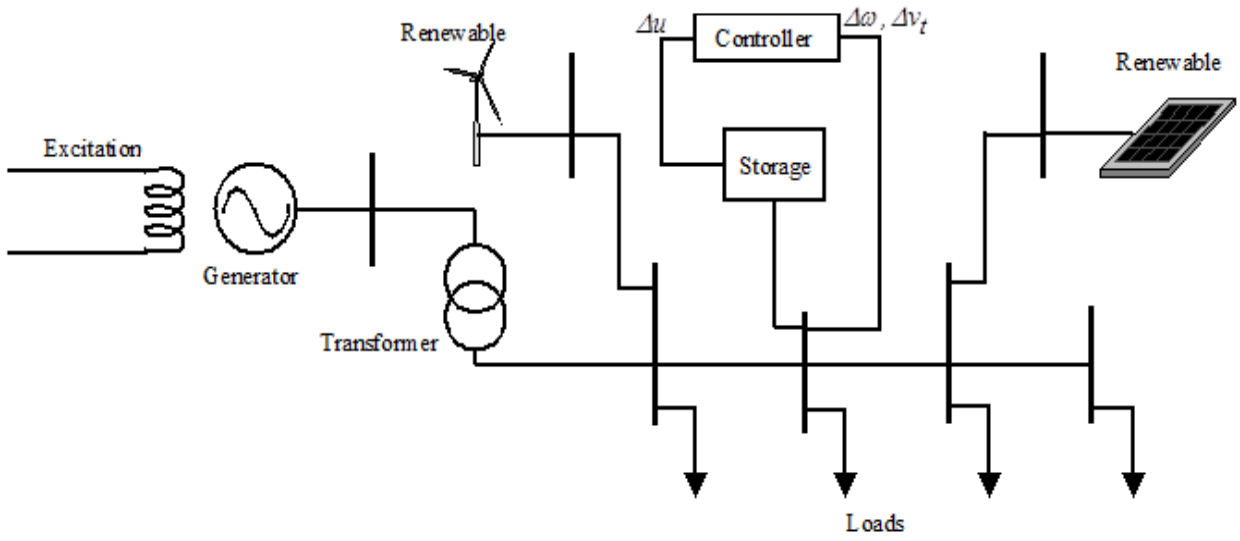


Figure 2.2 One-line diagram of the micro grid

## 2.1.Synchronous Generator Model

A synchronous machine can be defined by a set of n+1 equations, where n are electrical and one is mechanical. Figure 2.3 refers to the three-phase generator showing armature winding a, b, and c and Figure 2.4 portrays the equivalent circuit for reference phase a of the generator. Electrical equations are obtained by equating voltage at the winding's terminals to the sum of resistive and inductive voltage drops across the winding (Kirchhoff's Voltage Law) [30].

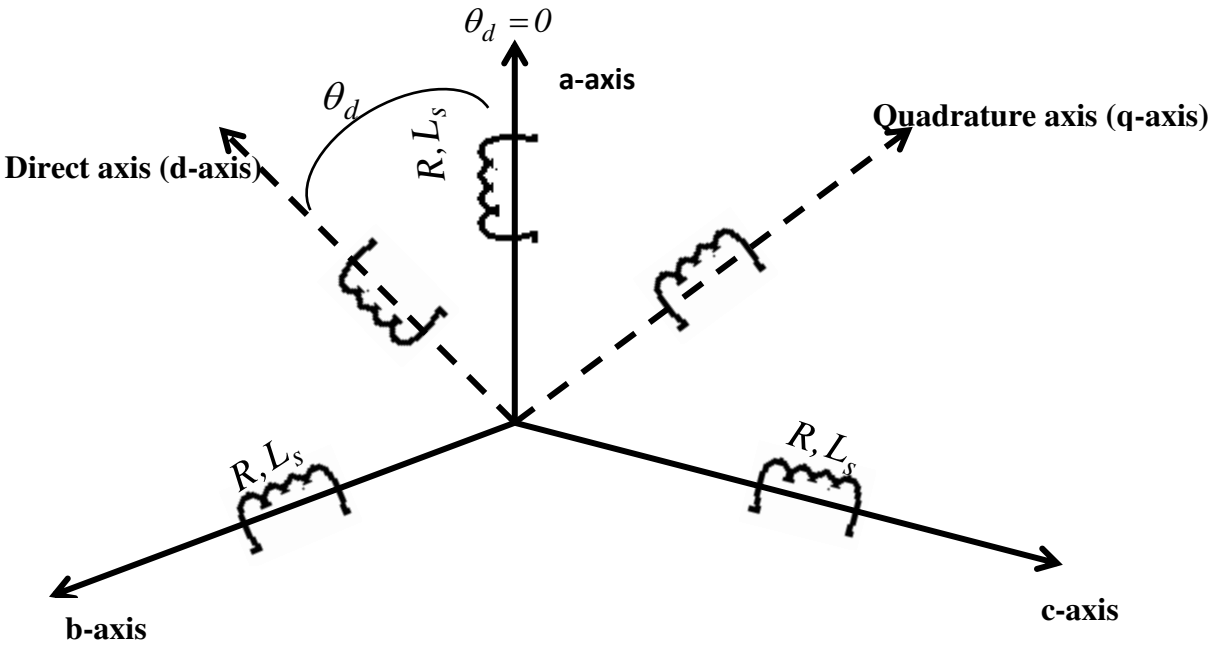


Figure 2.3 Synchronous generator three-phase winding

In Figure 2.4 below $X_d^{'}$ is the reactance of the winding. The generator is rotating at a synchronous speed $\omega$ and has the internal emf of $E_i$ and terminal voltage $V_a$. $\theta_d$ (Figure 2.3) indicates the position of the d-axis with respect to a-phase, and hence $\delta \approx \theta_d - 90°$ denotes the position of the q-axis. And finally, $I_a$ is the current in the phase-a with $\theta$ as the angle of lag of $I_a$ measured with respect to the terminal voltage $V_a$.

Similarly, the equations and equivalent circuits for phase b and phase c can be developed. However, the equations of asynchronous generator can be expressed in a much simpler form by transforming a, b, and c variables of the stator into direct-axis and quadrature-axis quantities [27].

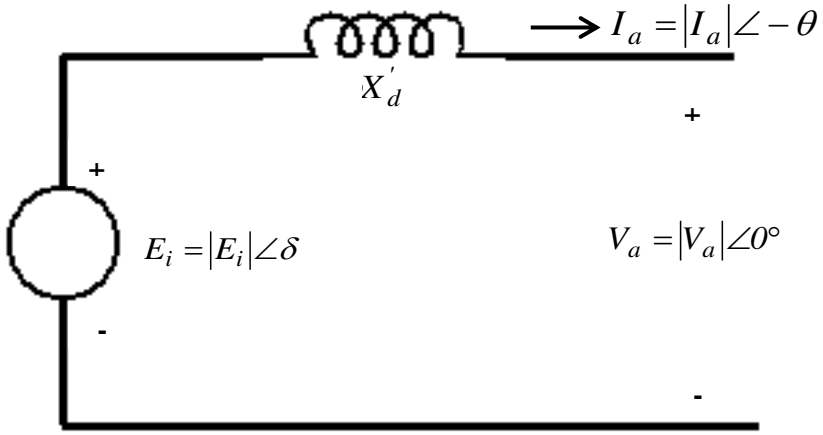


Figure 2.4 Equivalent circuit for reference phase-a of the synchronous generator showing voltages and currents.

This transformation is made possible by the matrix called Park's transformations such that $V_{dqo} = P.V_{abc}$ and $I_{dqo} = P.I_{abc}$ where $P$ is a 3-by-3 matrix given in (2.1) [27]

$$P = \sqrt{\frac{2}{3}} \begin{bmatrix} \cos\theta_d & \cos(\theta_d - 120°) & \cos(\theta_d - 240°) \\ \sin\theta_d & \sin(\theta_d - 120°) & \sin(\theta_d - 240°) \\ \frac{1}{\sqrt{2}} & \frac{1}{\sqrt{2}} & \frac{1}{\sqrt{2}} \end{bmatrix} \tag{2.1}$$

## 2.1.1 Design 1

We model the synchronous generator using the flux-decay model (one-axis model) given by the following equations [19] as

$$\dot{E}'_q = \frac{1}{T'_{do}} \left( -E'_q - \left( X_d - X'_d \right) I_d + E_{fd} \right) \tag{2.2}$$

$$\dot{\delta} = \omega_i - \omega_s \tag{2.3}$$

$$\dot{\omega} = \frac{\omega_s}{2H}\left(P_m - E_q^{'} I_q - \left(X_q - X_d^{'}\right) I_d I_q\right) \tag{2.4}$$

where $T_{do}^{'}$ is the direct axis open circuit transient time constant, $X_d$ is the direct axis synchronous reactance of the generator, $X_d^{'}$ is the direct axis transient reactance of the generator, $X_q$ is the quadrature axis synchronous reactance of the generator, $E_q^{'}$ is the instantaneous voltage proportional to the field flux linkage, $\delta$ is the rotor angle deviation, $E_{fd}$ is the field voltage, $P_m$ the mechanical input to the generator, $\omega$ is the angular speed, and $H$ is the machine inertia. $H$ is interpreted as the time the generator takes (in seconds) to reach standstill if the generator rotating at rated speed with rated load, is disconnected from the turbine [20] and can be defined in terms of inertia constant $M$ of the machine as in (2.5)

$$M = \frac{2H}{\omega_s}. \tag{2.5}$$

Figure 2.5 portrays the complex representation of the equivalent circuit of the flux-decay model of a synchronous generator where the voltage $E$ is given by (2.6)

$$\vec{E} = (X_q - X_d^{'}) I_q + jE_q^{'}. \tag{2.6}$$

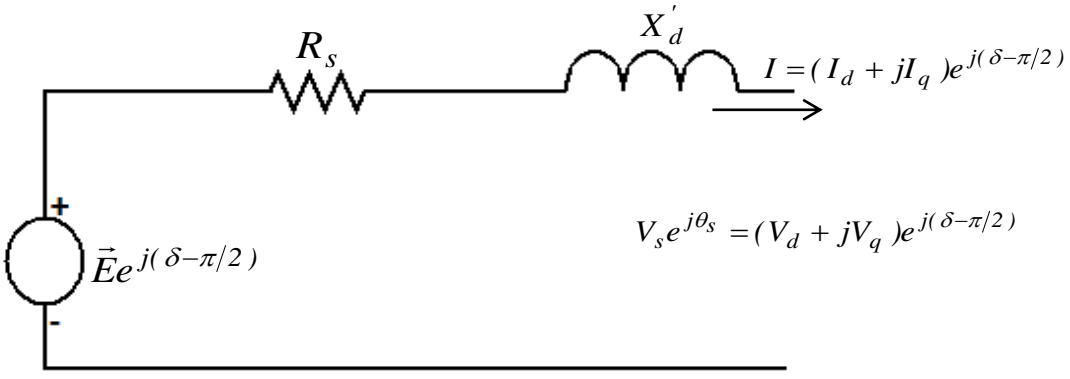


Figure 2.5 Complex representation of equivalent circuit of flux-decay model of synchronous generator

The following algebraic equations are used to express the model of the synchronous generator

$$0 = R_s I_d - X_q I_d + V_d \tag{2.7}$$

$$0 = R_s I_q - X_d^{'} I_d + V_q - E_q^{'} \tag{2.8}$$

$$0 = V_t^2 - \left(V_d^2 + V_q^2\right) \tag{2.9}$$

where $R_s$ is the stator resistance; $V_t$ is the terminal voltage; $I_d$ and $V_d$ denote d-axis stator current and voltage, respectively; and $I_q$ and $V_q$ are the q-axis stator current and voltage.

The synchronous generator is equipped with exciter, power system stabilizer (PSS), and governor as shown in Figure 2.6. These components help the power system to maintain constant voltages and to provide damping of the oscillation. The basic function of an exciter is to provide direct current to the synchronous machine field winding thereby inducing ac voltage and current in the generator's armature. The exciter provides the value $E_{fd}$, which is a scaled field voltage. The exciter provides an excitation system for synchronous generator and regulates its terminal voltage.

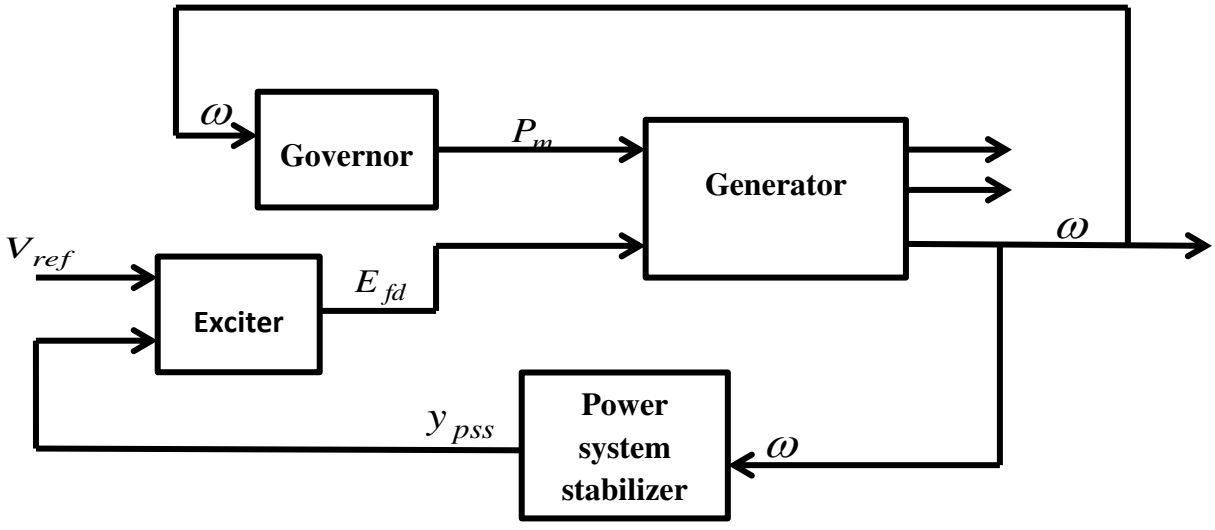


Figure 2.6 General functional block diagram for a synchronous generator

The exciter can be represented by following transfer function

$$E_{fd} = \frac{K_a}{s.T_a + 1}\left( - \frac{V_t}{s.T_r + 1} - \frac{E_{fd}.K_f}{s.T_f + 1} + y_{pss} + V_{ref} \right) \tag{2.10}$$

where $T_r$, $T_f$, and $T_a$ are time constants, $K_f$ and $K_a$ are the gains, and $y_{pss}$ is the stabilization signal used to control the terminal voltage $V_t$ of the generator. The block diagrams of exciter shown in Figure 2.7 reveals the inputs and outputs of the exciter used in this thesis. It feeds on terminal voltage signal obtained from the synchronous generator. $V_{ref}$ is the desired value of voltage, $y_{pss}$ is the voltage signal to provide additional stabilization of the oscillations. The state variables of the excitation system are represented by $X_1$ and $X_2$ in Figure 2.7

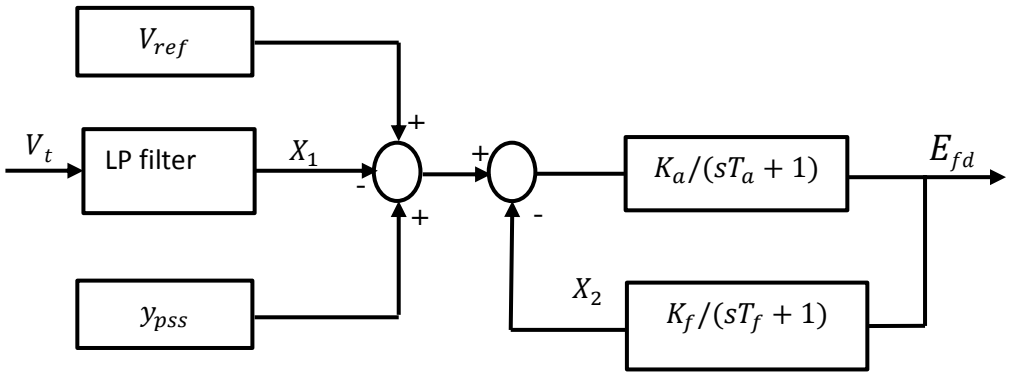


Figure 2.7 The excitation system of the generator

Next, the disturbances occurring in the power systems must be damped to maintain the system stability and the power system stabilizer does this by controlling its excitation [21]. The output of the PSS is used as an additional input ( $y_{pss}$ ) to the exciter as seen in Figure 2.7 and 2.8. The power system stabilizer is represented by the following block diagram in Figure 2.8 and the transfer function for PSS can be given by (2.11) as

$$\frac{y_{pss}}{\Delta\omega} = \left( \frac{s.T_{2n} + 1}{s.T_{2d} + 1} \right)\left( \frac{s.T_{1n} + 1}{s.T_{1d} + 1} \right)\left( \frac{1}{sT_s + 1} \right)\left( \frac{s}{sT_w + 1} \right) \tag{2.11}$$

where $T_s$ and $T_w$ are the sensor and washout time constants whereas $T_{1n}$, $T_{1d}$, $T_{2n}$, and $T_{2d}$ are lead and lag time constants. The state variables of the PSS are represented by $X_3$ through $X_5$ in Figure 2.8.

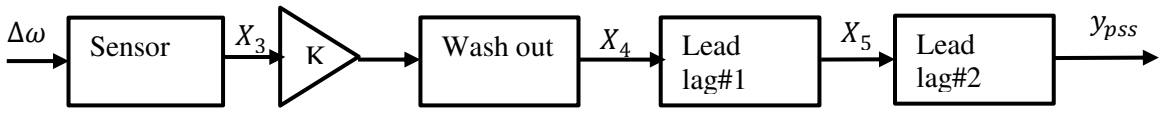


Figure 2.8 The Power System Stabilizer (PSS) of the generator

As seen in Figure 2.8, the PSS model consists of a sensor (low-pass filter), a general gain, a washout high-pass filter, and a phase-compensation system (lead-lag transfer functions). The generator's speed deviation signal is used as the input which passes through the first-order low-pass filter. The gain determines the amount of damping produced by the stabilizer. Then the first order washout high-pass filter attenuates the low frequencies that are present in the speed signal. Lastly, the two first-order lead lag transfer functions compensate the phase lag between the excitation voltage and torque of the generator [21].

Finally, the steam turbine governor is used to provide and control the mechanical power to the generator. The speed governing system consists of proportional regulator, speed relay, and servomotor while the steam turbine consists of steam chest and reheaters as shown in the block diagram of Figure 2.9. The governor and the turbine together are represented as (2.12)

$$\frac{P_m}{\Delta\omega} = \left(\frac{1}{sT_3+1}\right)\left(\frac{1}{sT_5+1}\right)\left(\frac{1}{sT_{sm}+1}\right)\left(\frac{1}{sT_{sr}+1}\right)\left(F_2\,\frac{1}{sT_4+1}+F_3\right) \tag{2.12}$$

where $T_{sr}$ and $T_{sm}$ are speed relay and servo motor time constants respectively while $T_3$, $T_4$, and $T_5$ are the steam turbine time constants, and $F_2$ and $F_3$ are turbine stages torque fractions. The speed relay is represented as an integrator with time constant $T_{sr}$ and the servomotor is characterized as an integrator with time constant $T_{sm}$. The steam turbine has four stages, each modeled by a first-order transfer function.

The first stage represents the steam chest while the three other stages represent reheaters. Turbine torque fractions $F_2$ to $F_3$ are used to distribute the turbine power to different shaft stages. All the torque from the turbine is added together and applied to the machine's mass and utilized to generate the mechanical power that is fed to the generator. The state variable of the turbine/governor are represented by $X_7$ through $X_{10}$ in Figure 2.9.

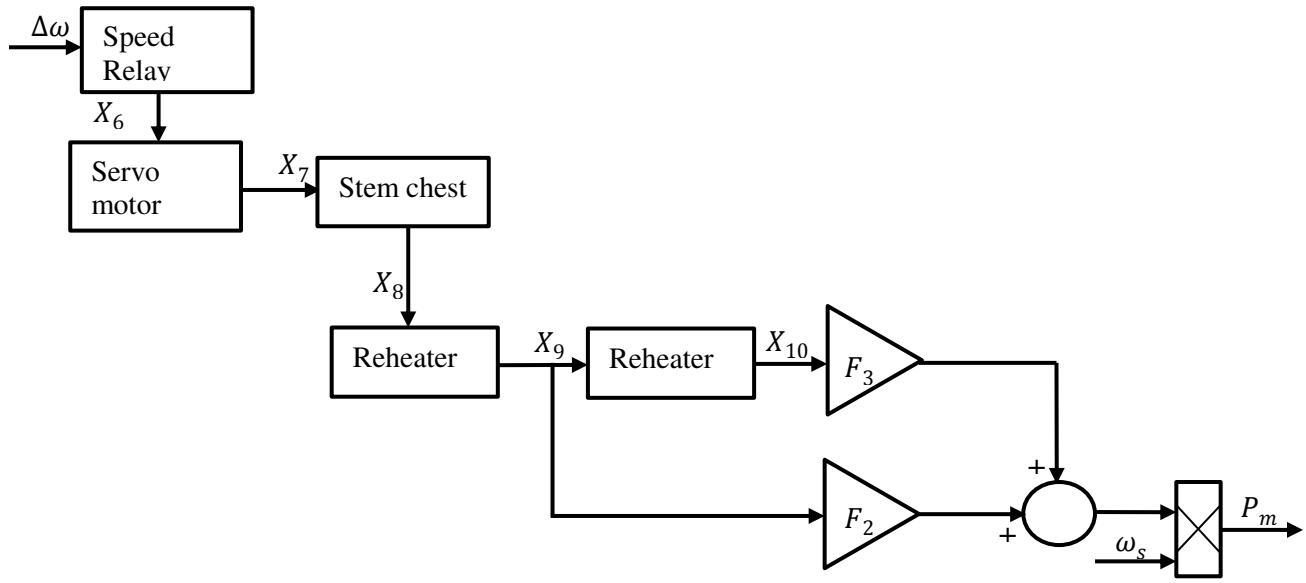


Figure 2.9 The Steam Turbine Governor of the generator.

## 2.1.2. Design 2

In the second design, we model the synchronous generator using the flux decay model similar to the first design.

However, we model the exciter, PSS, governor, and turbine as will be explained in the following where each component is represented by a different set of equations. The exciter has the following equations

$$\dot{E}_{fd} = \frac{1}{T_E}\left[-K_E E_{fd} + V_R\right] \tag{2.13}$$

$$\dot{V}_R = \frac{1}{T_A}\left[ K_A R_F - V_R - \frac{K_A K_F}{T_F} E_{fd} + K_A\left(V_{ref} - V_t + y_{pss}\right)\right] \tag{2.14}$$

$$\dot{R}_F = \frac{1}{T_F}\left[\frac{K_F}{T_F} E_{fd} - R_F\right] \tag{2.15}$$

where $V_R$ is normally the scaled output of the pilot exciter and is applied to the field of the separately excited main exciter, $T_A$, $T_E$, and $T_F$ are the time constants related to the exciter, $K_A$, and $K_f$ are gains, $V_{ref}$ is the desired value of stator terminal voltage, $y_{pss}$ is the voltage signal provided by PSS for additional stabilization of the oscillations, and $R_F$ ,and $V_R$ are the variable states associated with the exciter.

Next, the governor is modeled with the equations given in (2.16) to (2.18) as

$$\dot{T}_M = \frac{1}{T_{RH}}\left[ -T_M + \left(1 - K_{HP}\frac{T_{RH}}{T_{CH}}\right)P_{CH} + K_{HP}\frac{T_{RH}}{T_{CH}} P_{SV}\right] \tag{2.16}$$

$$\dot{P}_{CH} = \frac{1}{T_{CH}}\left(P_{SV} - P_{CH}\right) \tag{2.17}$$

$$\dot{P}_{SV} = \frac{1}{T_{SV}}\left[ P_C - P_{SV} - \frac{\omega_i}{\omega_s R_s}\right] \tag{2.18}$$

where $T_M$ is the synchronous machine's torque, $P_{CH}$ and $P_{SV}$ are the dynamic states of the turbine and steam value pressure, $K_{HP}$ is the gain, and $T_{HP}, T_{RH}, T_{CH}$ , and $T_{SV}$ are time constants.

Finally, the power system stabilizer for the new system can be denoted with the following equations (2.19) through (2.21) as

$$\dot{P}_1 = \frac{K_{PSS}}{T_s}\omega_i - \frac{P_1}{T_s} \tag{2.19}$$

$$\dot{P}_2 = \frac{-P_2}{T_w} + \dot{P}_1 \tag{2.20}$$

$$\dot{y}_{pss} = \frac{P_2}{T_2} - \frac{y_{pss}}{T_2} + \frac{T_1}{T_2}\dot{P}_2 \tag{2.21}$$

where $P_1$ and $P_2$ are the dynamic states of the PSS, $y_{pss}$ is the stabilizing voltage that is fed to the exciter, $K_{PSS}$ is the gain, $T_s$ and $T_w$ are sensor and wash out time constants, and $T_1$ and $T_2$ are the lead lag time constants.

## 2.2.Thermal Storage Model

In this thesis, following two types of thermal storage devices are proposed

1) Resistor type which uses resistive thermal elements to produce heat

2) Heat pump type (variable-voltage) that employs a compressor to provide hot or cold water (or any other suitable medium).

### 2.2.1. Resistor-type Thermal Storage

A resistor type thermal storage uses resistor thermal elements to produce heat. In the resistor type thermal storage, the consumed power in the thermal storage is controlled through changing the number of parallel resistors in a large array of resistors. This way, the storage power controller dynamically changes the total resistance (i.e., variable resistance) of the thermal element. Figure 2.10 shows such a figure with an array of resistors and switches.

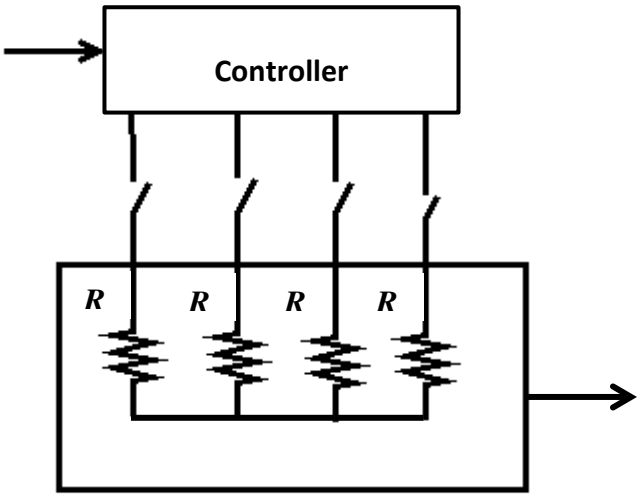


Figure 2.10 An array of resistors with switches and controller

In this case, power electronic equipment-the major source of harmonic distortion, is not required. The resistor type thermal storage is convenient in handling fast power transients caused by disturbances due to its faster dynamics. The resistor type thermal storage can also be used to mitigate slower power fluctuations caused by intermittent renewable energy sources. First, we develop the resistor type thermal storage model.

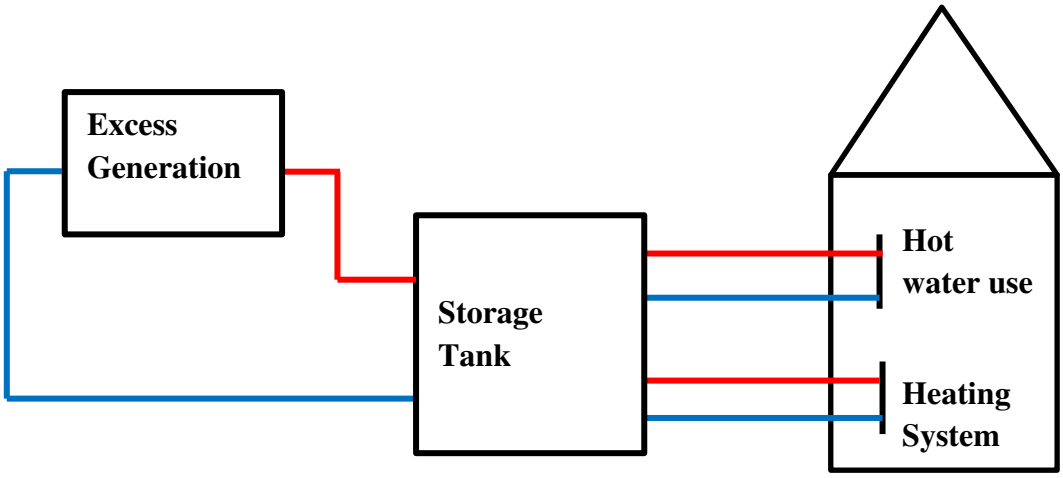


Figure 2.11 Example of thermal storage

The consumed power in resistor type storage is controlled by variable change in the resistance as explained. If $V_i$ is the voltage across the resistance *R*, power $P_{si}$ is given by $P_{si} = V_i^2 / R$ In other words, the total power absorbed by the resistor type storage is given by (2.22) as

$$P_{si} = G_{si} V_i^2 \; ; Q_{si} = 0 \tag{2.22}$$

where $G_{si}$ is the variable conductance $(G_{si} = 1/R)$ of the thermal storage. As the thermal storage will act as a controller to mitigate the system oscillations, the proposed method involves active power control of the generator using the thermal storage.

### 2.2.2. Heat Pump-type Thermal Storage

Heat pumps are systems that draw heat from one source and transfer to another. The heat pumps employ compressors to provide heat initially and are used to absorb heat from the cold environment and pump it to the warmer places [22]. Figure 2.12 illustrates an example of heat pump water storage [31].

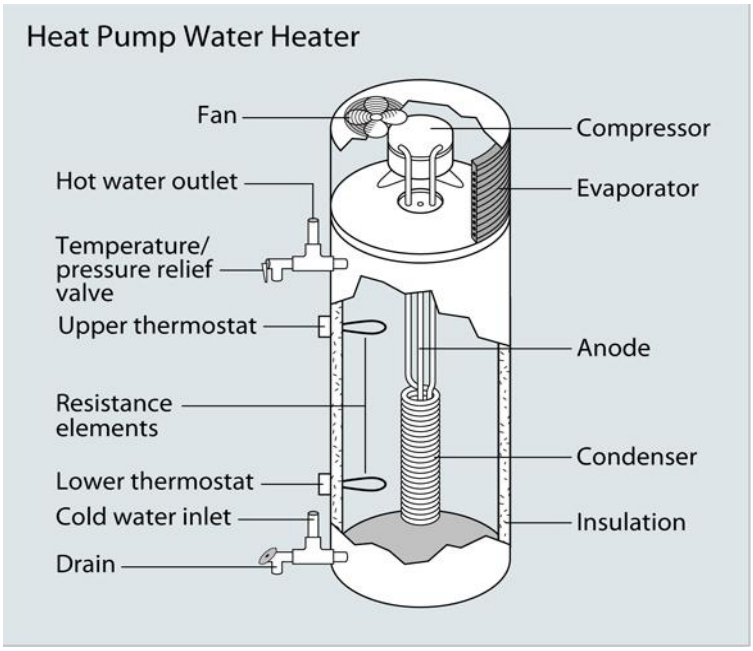


Figure 2.12 Diagram of heat pump water heater

The same device provides cold medium in cooling applications through the same phenomenon, and thus, in this thesis by heat pump we refer to heating or cooling equipment that employs a compressor.

Next, we develop the heat pump thermal storage model. The controlled element in the heat pump is the driving electric motor which is usually an induction motor. Figure 2.13 illustrates the equivalent circuit of an induction motor.

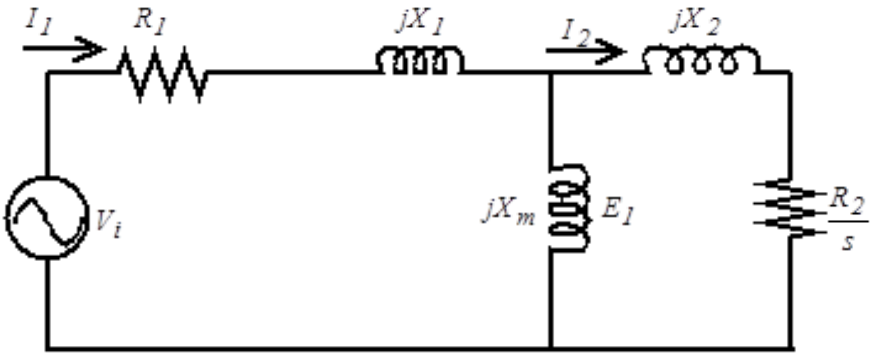


Figure 2.13 The equivalent circuit of an induction motor

Here $R_1$ and $X_1$ are the stator resistance and reactance, respectively, $R_2$ and $X_2$ the rotor resistance and reactance referred to the stator, respectively, and *s* is the slip of the induction motor. The induction motor simplified equivalent circuit is shown in Figure 2.14 where $R_{TH} + jX_{TH}$ the Thevenin equivalent impedance of the induction motor stator is, and $V_{TH}$ is the Thevenin equivalent voltage of the source seen from branch $E_1$.

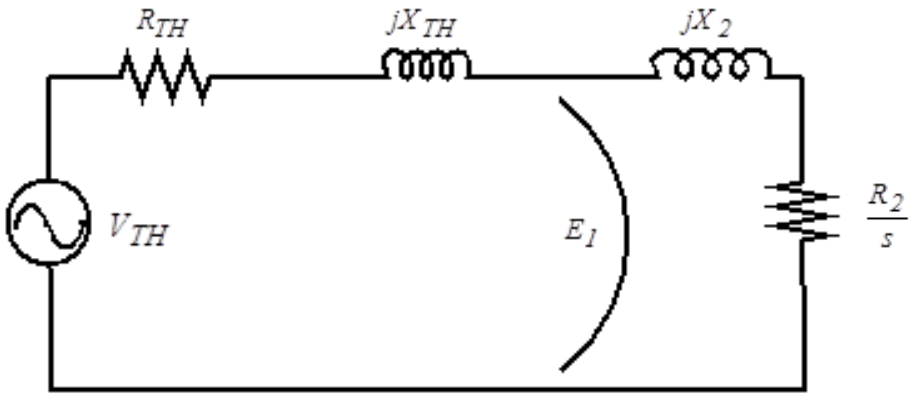


Figure 2.14 Thevenin equivalent circuit

From this circuit the current $I_2$ is given by (2.23)

$$I_2 = \frac{V_{TH}}{R_{TH} + R_2/s + jX_{TH} + jX_2} \ . \tag{2.23}$$

The magnitude of the Thevenin voltage can be approximately calculated in (2.24) as

$$V_{TH} \approx V_i \beta \frac{X_m}{X_1 + X_m} \tag{2.24}$$

where $\beta$ is the square of the autotransformer turns ratio and $V_i$ is the terminal voltage. The magnitude of the current in (2.23) can be obtained in (2.25) as

$$|I_2| = \frac{V_{TH}}{\sqrt{(R_{TH} + R_2/s)^2 + (X_{TH} + X_2)^2}} \ . \tag{2.25}$$

If $P_{si}$ and $Q_{si}$ are the three-phase active and reactive power absorbed by the induction motor, then, they are approximately given by (2.26) and (2.27) as

$$P_{si} = 3|I_2|^2 \frac{R_2}{s} \tag{2.26}$$

and

$$Q_{si} = 3|I_2|^2 (X_{TH} + X_2) \ . \tag{2.27}$$

From (2.25), (2.26), and (2.27), we obtain the following expressions for the power

$$P_{si} = \frac{3V_{TH}{}^2 R_2/s}{(R_{TH} + R_2/s)^2 + (X_{TH} + X_2)^2} = K_p \beta V_i{}^2 = G_{si} V_i{}^2 \tag{2.28}$$

$$Q_{si} = \frac{3V_{TH}{}^2 (X_2 + X_{TH})}{(R_{TH} + R_2/s)^2 + (X_{TH} + X_2)^2} = K_q \beta V_i{}^2 = B_{si} V_i{}^2 \tag{2.29}$$

where

$$K_p = \frac{3\beta X_m{}^2 R_2/s}{\left((R_{TH} + R_2/s)^2 + (X_{TH} + X_2)^2\right)(X_1 + X_m)^2} \tag{2.30}$$

$$K_q = \frac{3\beta X_m{}^2 (X_2 + X_{TH})}{\left((R_{TH} + R_2/s)^2 + (X_{TH} + X\ \ )^2\right)(X_1 + X_m)^2}\ . \tag{2.31}$$

By assuming that the induction motor responds to the heat pump load changes under variable voltage and constant slip, $K_p$ and $K_q$ become constant. Such an assumption is valid under slow dynamics of heat pump load and the controller to accommodate the intermittent slow changes (in the range of a few seconds and longer) in the renewable sources' generated power compared to the fast transients of the faults (less than a second.) Hence, in the simulation sections we have compared the result of heat pump to that of the PSS only in the case of slow power changes due to renewables. From equations (2.28) and (2.29), we conclude (2.32) as [23]

$$\frac{Q_{si}}{P_{si}} = \frac{B_{si}}{G_{si}} = \frac{K_q}{K_p} = \frac{(X_2 + X_{TH})s}{R_2} \tag{2.32}$$

where $G_{si}$ and $B_{si}$ are the conductance and susceptance of the heat pump type thermal storage, respectively.

## 2.3.Power Balance Equations

The power flow study must be performed on a power system to obtain the voltage angle and magnitude information at each bus in the power system. The power flow helps to determine the values of all state (or dependent) variables by solving the power flow equations [24]. Once all the states of the

system is identified (i.e., all voltage angles and magnitudes as well as generator dynamics) all other quantities, which depend on the state variables, can be established and a stabilizing controller for the system can be designed. Since the power balance equations are non-linear functions, iterative methods like Newton-Raphson are used to solve the power balance equations.

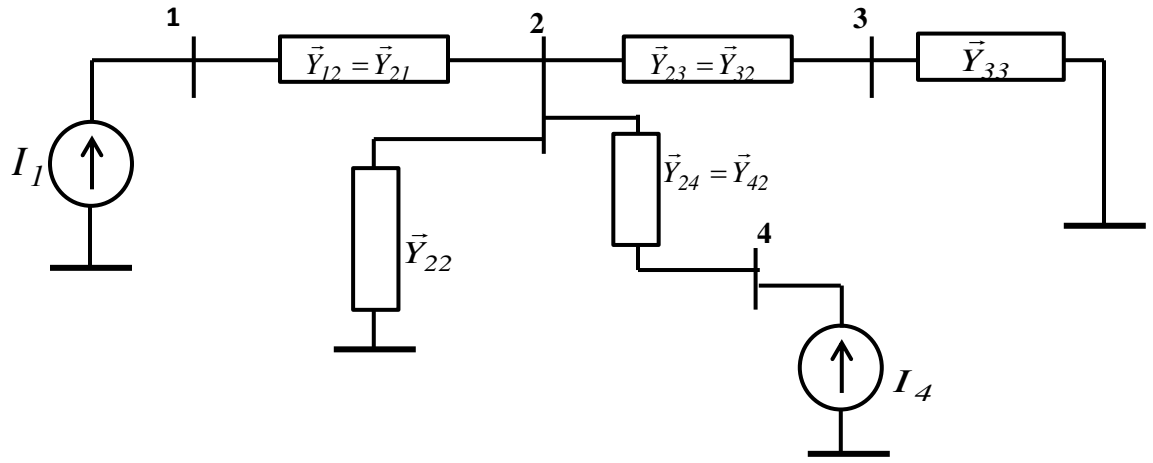


Figure 2.15 A generic power system network

A generic power system topology is given in Figure 2.15 where the powers are distributed among the buses based on the amount of generation and load in the entire system. For such a power system, the admittance matrix can be developed using Kirchhoff's Current Law (KCL) as [27]

$$-\vec{I}_1 + \vec{Y}_{12}(\vec{V}_1 - \vec{V}_2) = 0$$

$$\vec{Y}_{21}(\vec{V}_2 - \vec{V}_1) + \vec{V}_2\vec{Y}_{22} + \vec{Y}_{23}(\vec{V}_2 - \vec{V}_3) + \vec{Y}_{24}(\vec{V}_2 - \vec{V}_4) = 0 \tag{2.33}$$

$$\vec{Y}_{32}(\vec{V}_3 - \vec{V}_{12}) + \vec{V}_3\vec{Y}_{33} = 0$$

$$-\vec{I}_4 + \vec{Y}_{42}(\vec{V}_4 - \vec{V}_2) = 0$$

In matrix form

$$\begin{bmatrix} \vec{I}_1 \\ 0 \\ 0 \\ \vec{I}_4 \end{bmatrix} = \begin{bmatrix} \vec{Y}_{12} & -\vec{Y}_{12} & 0 & 0 \\ -\vec{Y}_{21} & \vec{Y}_{21} + \vec{Y}_{22} + \vec{Y}_{23} & -\vec{Y}_{23} & 0 \\ 0 & -\vec{Y}_{32} & \vec{Y}_{32} + \vec{Y}_{33} & 0 \\ 0 & -\vec{Y}_{42} & 0 & \vec{Y}_{42} \end{bmatrix} \times \begin{bmatrix} \vec{V}_1 \\ \vec{V}_2 \\ \vec{V}_3 \\ \vec{V}_4 \end{bmatrix} \tag{2.34}$$

Now for an M-bus system, if *i* and *j* are the bus numbers based on equation (2.34) we can define

$\vec{Y}_{ij} = \vec{Y}_{ji} = \dfrac{-1}{Z_{ij}}$ for $i \neq j$ and $, \vec{Y}_{ij} = Y_{ij} \angle \phi_{ij}$ where $Z_{ij}$ is the impedance between bus *i* and bus $j$

$$\vec{Y}_{ii} = \sum_{\substack{k=1 \\ k \neq i}}^{M} \frac{1}{Z_{ik}} = Y_{ii} \angle \phi_{ii}$$

where $Z_{ik}$ is the impedance connected between bus *i* and bus *k.*

From the definitions above the currents can be obtained as (2.35)

$$\vec{I} = Y_{bus} . \vec{V} \tag{2.35}$$

Now, the power balance equations for the generator bus *i* (*i*=generator bus number); that is, the voltage controlled buses are given in (2.36) as

$$\begin{aligned} 0 &= V_{di} I_{di} + V_{qi} I_{qi} - V_i \sum_{j=1}^{N} V_j Y_{ij} \cos\left(\theta_i - \theta_j - \phi_{ij}\right) - P_{Li} \\ 0 &= V_{qi} I_{di} - V_{di} I_{qi} - V_i \sum_{j=1}^{N} V_j Y_{ij} \sin\left(\theta_i - \theta_j - \phi_{ij}\right) - Q_{Li} \end{aligned} \tag{2.36}$$

where $P_{Li}$ and $Q_{Li}$ are the active and reactive power associated with the loads; $Y_{ij}$ is the admittance between bus *i* and *j,* $\theta_i$, and $\theta_j$ are the angles of bus voltages $V_i$ and $V_j$, respectively, $\phi_{ij}$ is the angle associated with $Y_{ij}$, and *N* is the total number of buses. Since the proposed micro grid has only one synchronous generator, the index *i* may be omitted. The power balance equations for load buses or the non-generator buses (*i*=load bus number) can be given by (2.37) as

$$\begin{aligned} 0 &= -V_i \sum_{j=1}^{N} V_j Y_{ij} \cos\left(\theta_i - \theta_j - \phi_{ij}\right) - P_{Li} \\ 0 &= -V_i \sum_{j=1}^{N} V_j Y_{ij} \sin\left(\theta_i - \theta_j - \phi_{ij}\right) - Q_{Li} \end{aligned} \quad . \tag{2.37}$$

## 2.4.Renewable Energy Source Model

Since there is no control on the power generated by the renewable sources and these sources are connected to the micro grid through power electronics, they are modeled as variable generations where their powers vary with the ambient energy variations such as changes in the wind speed or the solar radiation. Thus, the renewable sources can be modeled by power balance equations (i=renewable bus number) given in (2.38) as

$$\begin{aligned} 0 &= -V_i \sum_{j=1}^{N} V_j Y_{ij} \cos\left(\theta_i - \theta_j - \phi_{ij}\right) + P_{Ri} \\ 0 &= -V_i \sum_{j=1}^{N} V_j Y_{ij} \sin\left(\theta_i - \theta_j - \phi_{ij}\right) + Q_{Ri} \end{aligned} \tag{2.38}$$

where and are the active and reactive generated powers by the renewable sources and subject to change as the ambient energy change.

# CHAPTER 3
# CONTROLLER DESIGN

This chapter concentrates on the controller design of the proposed storage to improve the system oscillations. The purpose of this chapter is to employ the state space representation of the power systems and the linear quadratic regulator (LQR) optimal controller to control the system oscillations with the help of the obtained state space representation.

The goal of the control in this thesis is to employ the storage's active power as a means of power flow control and improving the micro grid stability, and thus, provide a damping controller to smooth the power oscillations when disturbances occur due to fault or load change or renewable energy fluctuation. In this thesis the controller design is obtained through linearization technique. In order to design the controller with linearization techniques, the sate space representation is used to model the power systems and their control inputs.

The control input signal for the proposed micro grid is the conductance of the resistive thermal storage $u = G_{si}$ . As mentioned in the previous chapter, the micro grid is described by a set of differential-algebraic equations, where differential equations represent the synchronous generator dynamics and the algebraic equations describe the power balance in the micro grid as shown in equations (2.2) through (2.12) for Design 1 and (2.13) through (2.21) for Design 2 followed by (2.34) through (2.36) for both the models. In order to design a proper controller we employ the linearization techniques to reduce the differential-algebraic equations mentioned in the previous section to purely differential equations [26] as explained in the following.

## 3.1. Linearization of Differential and Algebraic Equations of Design 1

The generator differential equations (2.2) through (2.4) are linearized around the equilibrium (operating) point in the micro grid as shown in the following equations (3.1) through (3.3) as

$$\Delta \dot{E}_q^{'} = \frac{-1}{T_{do}^{'}} \Delta E_q^{'} - \frac{1}{T_{do}^{'}} \left( X_d - X_d^{'} \right) \Delta I_d + \frac{1}{T_{do}^{'}} \Delta E_{fd} \tag{3.1}$$

$$\Delta\dot{\delta} = \Delta\omega_i \tag{3.2}$$

$$\Delta\dot{\omega} = \frac{\omega_s}{2H}\Delta P_m - \frac{\omega_s}{2H} I_q \Delta E_q^{'} - \frac{\omega_s}{2H} E_q^{'} \Delta I_q - \frac{\omega_s}{2H}\left(X_q - X_d^{'}\right) I_q \Delta I_d - \frac{\omega_s}{2H}\left(X_q - X_d^{'}\right) I_d \Delta I_q . \tag{3.3}$$

The exciter reference voltage $\Delta V_{ref}$ (shown in Figure 2.7) is considered constant for the control design; hence $\Delta\dot{V}_{ref} = 0$. Then, the differential equations (2.10) through (2.12) regarding the governor and power system stabilizer are linearized as (3.4) through (3.15)

$$\Delta\dot{X}_1 = \frac{-1}{T_r}\Delta X_1 + \frac{\Delta V_{ref}}{Tr} = -\frac{1}{T_r}\Delta X_1 \tag{3.4}$$

$$\Delta\dot{X}_2 = \frac{-1}{T_f}\Delta X_2 + \frac{K_f}{T_f}\Delta E_{fd} \tag{3.5}$$

$$\Delta\dot{E}_{fd} = \frac{\Delta E_{fd}}{T_a} + \frac{K_a}{Ta}\Delta y_{pss} - \frac{K_a}{Ta}\Delta X_1 - \frac{K_a}{Ta}\Delta X_2 + \frac{K_a}{Ta}\Delta V_{ref} \tag{3.6}$$

$$\Delta\dot{X}_3 = \frac{\Delta X_3}{T_s} + \frac{\Delta\omega}{T_s} \tag{3.7}$$

$$\Delta\dot{X}_4 = \frac{-1}{T_w}\Delta X_4 + K\Delta\dot{X}_3 \tag{3.8}$$

$$\Delta\dot{X}_5 = \frac{-1}{T_{1d}}\Delta X_5 + \frac{\Delta X_4}{T_{1d}} + \frac{T_{1n}}{T_{1d}}\Delta\dot{X}_4 \tag{3.9}$$

$$\Delta\dot{y}_{pss} = \frac{-\Delta y_{pss}}{T_{2d}} + \frac{\Delta X_5}{T_{2d}} + \frac{T_{2n}}{T_{2d}}\Delta\dot{X}_5 \tag{3.10}$$

$$\Delta\dot{X}_6 = \frac{-\Delta X_6}{T_{sr}} + \frac{\Delta\omega}{T_{sr}} \tag{3.11}$$

$$\Delta\dot{X}_7 = \frac{-\Delta X_7}{T_{sm}} + \frac{\Delta X_6}{T_{sm}} \tag{3.12}$$

$$\Delta\dot{X}_8 = \frac{-\Delta X_8}{T_3} + \frac{\Delta X_7}{T_3} \tag{3.13}$$

$$\Delta\dot{X}_9 = \frac{-\Delta X_9}{T_4} + \frac{\Delta X_8}{T_4} \tag{3.14}$$

$$\Delta\dot{X}_{10} = \frac{-\Delta X_{10}}{T_5} + \frac{F_2}{T_5}\Delta X_9 + F_3\Delta X_9 + F_3\Delta\dot{X}_9 \ . \tag{3.15}$$

Next, the linearized form of the algebraic equations (2.6) through (2.9) of the generator is as given in (3.16) through (3.19)

$$0 = R_s\Delta I_d - X_q\Delta I_q + \Delta V_d \tag{3.16}$$

$$0 = R_s\Delta I_q + X'_d\,\Delta I_d + \Delta V_q - \Delta E'_q \tag{3.17}$$

$$0 = 2V_i\Delta V_i - (\,2V_d\Delta V_d + 2V_q\Delta V_q\,) \tag{3.18}$$

$$0 = \Delta V_q - cos(\,\delta-\theta\,)\Delta V_i + V_i\ sin(\,\delta-\theta\,)\Delta\delta - V_i\ sin(\,\delta-\theta\,)\Delta\theta \ . \tag{3.19}$$

## 3.2. Linearization of Differential Equations of Design 2

The differential equations (2.13) through (2.21) regarding the exciter, governor, and power system stabilizer are linearized around the equilibrium (operating) point as shown in (3.20) through (3.28)

$$\Delta\dot{E}_{fd} = \frac{K_E}{T_E}\Delta E_{fd} + \frac{\Delta V_R}{T_E} \tag{3.20}$$

$$\Delta\dot{V}_R = \frac{K_A}{T_A}\Delta R_F - \frac{1}{T_A}\Delta V_R - \frac{K_A K_F}{T_A T_F}\Delta E_{fd} - \frac{K_A}{T_A}\Delta V_t + \frac{K_A}{T_A}\Delta y_{pss} \tag{3.21}$$

$$\Delta\dot{R}_F = \frac{K_F}{T_F T_F}\Delta E_{fd} - \frac{1}{T_F}\Delta R_F \tag{3.22}$$

$$\Delta\dot{T}_M = \frac{-\Delta T_M}{T_{RH}} + \left(\frac{1}{T_{RH}} - \frac{K_{HP}}{T_{CH}}\right)\Delta P_{CH} + \frac{K_{HP}}{T_{CH}}\Delta P_{SV} \tag{3.23}$$

$$\Delta\dot{P}_{CH} = \frac{\Delta P_{SV}}{T_{CH}} - \frac{1}{T_{CH}}\Delta P_{CH} \tag{3.24}$$

$$\Delta\dot{P}_{SV} = \left[\frac{P_C}{T_{SV}} - \frac{1}{T_{SV}}\Delta P_{SV} - \frac{\Delta\omega_i}{T_{SV}\omega_s R_s}\right] \tag{3.25}$$

$$\Delta\dot{P}_1 = \frac{K_{PSS}\Delta\omega_i}{T_s} - \frac{\Delta P_1}{T_S} \tag{3.26}$$

$$\Delta\dot{P}_2 = \frac{-\Delta P_2}{T_w} + \Delta\dot{P}_1 \tag{3.27}$$

$$\Delta\dot{y}_{pss} = \frac{\Delta P_2}{T_2} - \frac{\Delta y_{pss}}{T_2} + \Delta\dot{P}_2\frac{T_1}{T_2}\ . \tag{3.28}$$

### 3.3. Linearization of Power Balance Algebraic Equations

Now, the power balance algebraic equations are linearized as

$$\begin{aligned}
0 = {} & I_d\Delta V_d + V_d\Delta I_d + I_q\Delta V_q + V_q\Delta I_q - V_i\sum_{\substack{j=1\\ j\neq i}}^{N} Y_{ij}\cos(\theta_i-\theta_j-\phi_{ij})\Delta V_j \\
& - \Delta V_i\sum_{\substack{j=1\\ j\neq i}}^{N} Y_{ij}\cos(\theta_i-\theta_j-\phi_{ij})V_j - 2V_iY_{ii}\cos\phi_{ij}\Delta V_i - V_i\sum_{\substack{j=1\\ j\neq i}}^{N} V_jY_{ij}\sin(\theta_i-\theta_j-\phi_{ij})\Delta\theta_j \\
& + V_i\sum_{\substack{j=1\\ j\neq i}}^{N} V_jY_{ij}\sin(\theta_i-\theta_j-\phi_{ij})\Delta\theta_i
\end{aligned} \tag{3.29}$$

$$\begin{aligned}
0 = {} & I_d\Delta V_q + V_q\Delta I_d - I_q\Delta V_d - V_d\Delta I_q - V_i\sum_{\substack{j=1\\ j\neq i}}^{N} Y_{ij}\sin(\theta_i-\theta_j-\phi_{ij})\Delta V_j \\
& - \Delta V_i\sum_{\substack{j=1\\ j\neq i}}^{N} Y_{ij}\sin(\theta_i-\theta_j-\phi_{ij})V_j + 2V_iY_{ii}\sin\phi_{ij}\Delta V_i + V_i\sum_{\substack{j=1\\ j\neq i}}^{N} V_jY_{ij}\cos(\theta_i-\theta_j-\phi_{ij})\Delta\theta_j \\
& - V_i\sum_{\substack{j=1\\ j\neq i}}^{N} V_jY_{ij}\sin(\theta_i-\theta_j-\phi_{ij})\Delta\theta_i
\end{aligned}$$

Here, for simplicity of the controller design, we restrict our design to the case with constant loads in the modeling section; however, the method is evaluated using variable loads as well. Finally, the

resistor type thermal storage, as explained by equation (2.22), is modeled by a variable conductance and the consumed power is controlled through changing the conductance for which a linearized model is obtained as

$$\Delta P_{si} = V_i^2 \Delta G + 2GV_i \Delta V_i . \tag{3.30}$$

For the heat pump type thermal storage, the active power is controlled via changing the square of autotransformer turns ratio $\beta$ as shown in equations (2.26) and (2.27) which leads to the linearized representation as

$$\Delta P_{si} = K_p V_i^2 \Delta\beta + 2K_p \beta V_i \Delta V_i = V_i^2 \Delta G + 2GV_i \Delta V_i \tag{3.31}$$

$$\Delta Q_{si} = K_q V_i^2 \Delta\beta + 2K_q \beta V_i \Delta V_i = V_i^2 \Delta B + 2BV_i \Delta V_i \ . \tag{3.32}$$

Thus, control signal can be essentially produced similarly for the two storage types.

### 3.4. State Space Model

The vectors of states and algebraic variables are defined as the changes in the actual variables around the equilibrium $x_e$ and the states of topology 1 are shown in (3.33) and (3.34) as

$$\Delta x = [\, \Delta E_q^{'}, \Delta\delta, \Delta\omega, \Delta X_1, \Delta X_2, \Delta E_{fd}, \Delta X_3, \Delta X_4, \Delta X_5, \Delta y_{pss}, \Delta X_6, \Delta X_7, \Delta X_8, \Delta X_9, \Delta X_{10} \,]^T \tag{3.33}$$

$$\Delta y = [\, \Delta I_d, \Delta I_q, \Delta V_d, \Delta V_q, \Delta\theta_1, \Delta V_1 ... \Delta\theta_n, \Delta V_N \,]^T \tag{3.34}$$

where $\Delta y_{pss}$ is the stabilization signal from the power system stabilizer, $\Delta X_1$ and $\Delta X_2$ are the states of the exciter, $\Delta X_3$, $\Delta X_4$, and $\Delta X_5$ are the states associated with the power system stabilizer, and $\Delta X_6$, $\Delta X_7$, $\Delta X_8$, $\Delta X_9$, and $\Delta X_{10}$ are the states of the steam turbine governor as shown in Figures 2.7, 2.8, and 2.9. The dynamic states of the second micro grid model can also be defined in a similar manner as (3.33) and (3.34). Consequently, from the linearized equations (3.1) through (3.19) and (3.29) through (3.32), the system can be represented by the following set of dynamic equations

$$\Delta\dot{x} = A_1\Delta x + B_1\Delta y + C_1\Delta u \tag{3.35}$$

$$0 = C\Delta x + D\Delta y + E\Delta u \tag{3.36}$$

where $\Delta u = \Delta G_{si}$ when the storage is of resistive type and $\Delta u = \Delta\beta$ when the storage is variable-voltage type. In these expressions $A_1, B_1, C_1, C, D,$ and $E$ represent the corresponding system matrices obtained by arranging the coefficients considering equations (3.1) through (3.30). By solving (3.36) for $\Delta y$ and replacing it in (3.35) we obtain

$$\Delta\dot{x} = A\Delta x + B\Delta u \ . \tag{3.37}$$

Equation (3.37) represents the state space model for the micro grid for which a proper stabilizing controller $\Delta u$ is to be developed.

To obtain an optimal control, one tends to find a controller that provides the best possible performance with respect to some given measure of performance [28]. Here in this thesis, the linear quadratic regulator (LQR) optimal controller is chosen to control the speed oscillations in micro grid due to guaranteed performance of such controllers and their robustness. According to the optimal control theory, the LQR, through an optimal state feedback, tends to minimize a quadratic cost function of the control input and the state variables, and thus, reach the steady state condition with minimum cost [26]. Figure 3.1 illustrates the LQR optimal control system configuration and the section below describes the function of LQR controller.

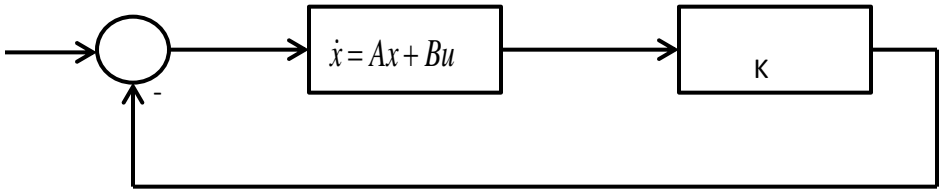


Figure 3.1 Linear Quadratic Regulator (LQR) feedback configuration

Consider the continuous-time linear system described by the following state space representation

$$\dot{x} = Ax + Bu \tag{3.38}$$

and the proposed cost function $J$ as

$$J = \int_0^\infty \left( x^T Q x + u^T R u \right) dt \tag{3.39}$$

where $Q$ and $R$ are positive-definite real symmetric matrices.

The optimal feedback control law that minimizes the value of the cost function $J$ is obtained as

$$u = -Kx \ . \tag{3.40}$$

In equation (3.40) K is defined as

$$K = R^{-1} B^T P \tag{3.41}$$

where $P$ is found by solving the continuous-time algebraic Riccati equation [26] as

$$A^T P + PA - PBR^{-1} B^T P + Q = 0 \, . \tag{3.42}$$

In the proposed micro grid, the appropriate $K$ is obtained using system (3.41) to minimize the cost function

$$J = \int_0^\infty \left( \Delta x^T Q \Delta x + R \Delta u^2 \right) dt \, . \tag{3.43}$$

In order to build a proper controller for the system, the states $\Delta X$ in (3.33) must be available. The required states can be directly measured or reproduced using an observer. In Design 1, by using the observer the states are reproduced (as seen in Figure 3.2) using the micro grid model introduced in the equations (3.41) in the neighborhood of the equilibrium $x_e$ , and thus, need not be measured. In other

words, from equations (2.2) through (2.11) and Figures 2.7, 2.8, and 2.9, it is observed that all the components of vector $\Delta X$ can be obtained from the measured speed $\omega$ and the generator voltage $V_t$ (Figure 2.7). However, the generator voltage might be unavailable to the controller due to possibly long distance. Though the generator voltage is different from that of the storage bus, the measured thermal storage bus voltage can be utilized and considered to be equal to the generator voltage and fed into the controller instead, which will cause an acceptable error. Hence, the controller produces the input $\Delta u$, which is used to control the thermal storage power. However in Design 2, as shown in Figure 3.3, the states are directly measured and fed through the controller to produce the input $\Delta u$.

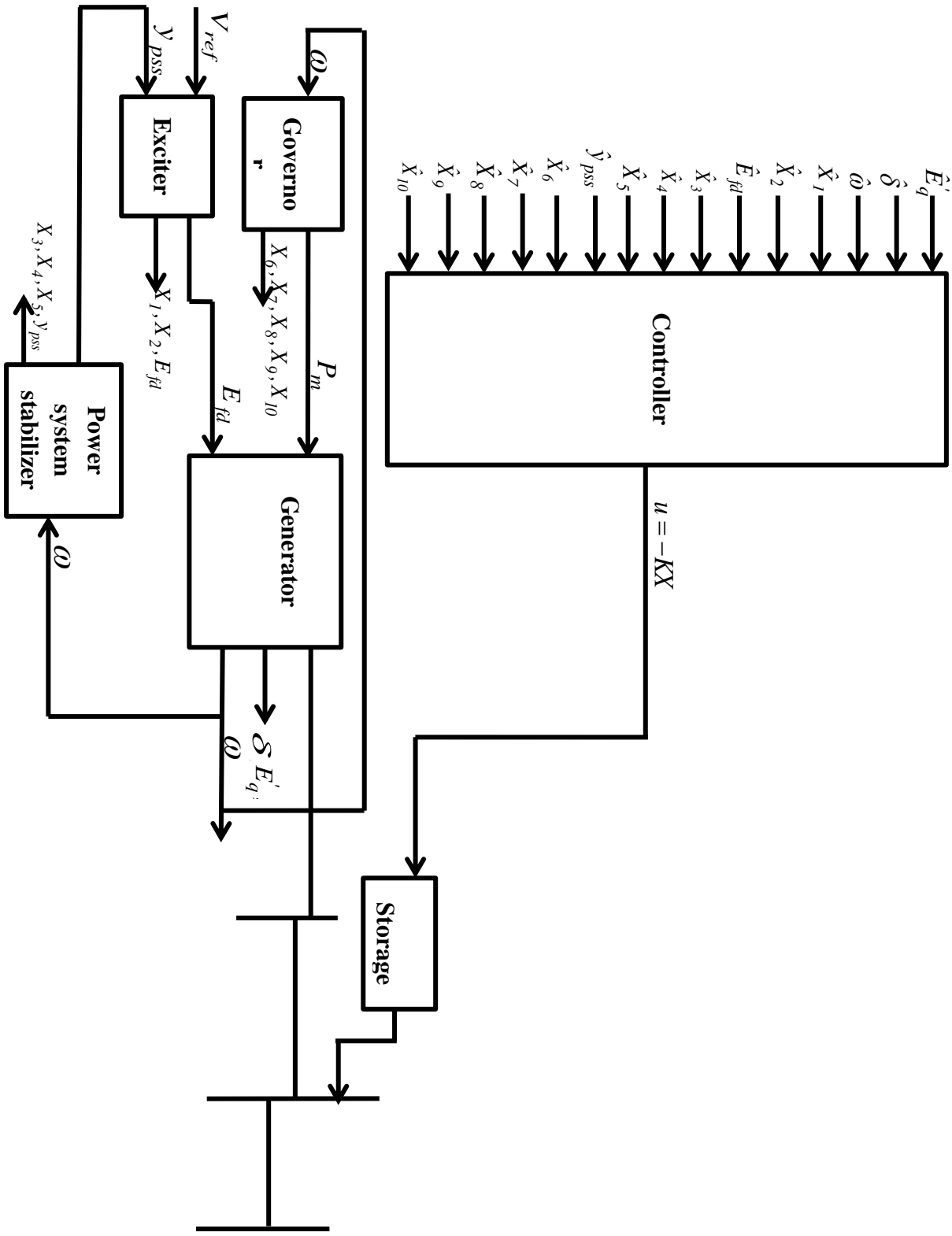


Figure 3.2 Functional block diagram of a micro grid model with observer.

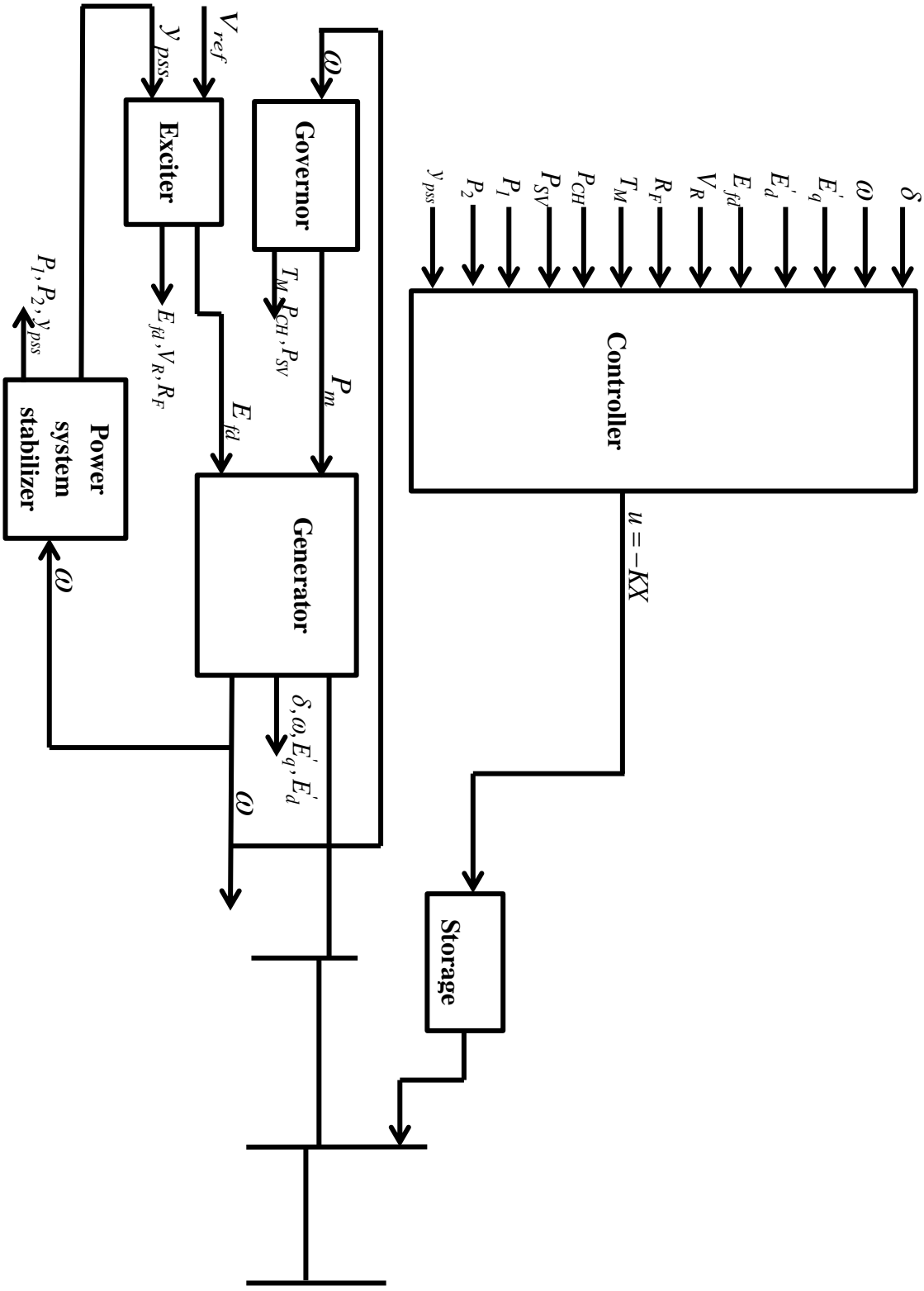


Figure 3.3 Functional block diagram of a micro grid model without observer

# CHAPTER 4
# SIMULATION RESULTS

This chapter discusses the different results obtained through simulations. The effort of this chapter is to demonstrate that the storage can conveniently provide effective stabilizing mechanism and demand response.

For validation of our theory two power system topologies are considered. In both cases the simulations are performed for various conditions in this section to evaluate the effectiveness of the storage and the proposed controller design. The micro grid is considered to be a city or a few neighborhoods in a large city powered majorly by a local power plant and is depicted in Figure 4.2.

## 4.1. Simulation Example 1

For our first simulation the system in Figure 4.1 is designed. The system is built in MATLAB/Simulink and consists of a 600MW synchronous generator to provide power at 22 kV. The generator models either a single large generator or an aggregation of a few small generators in a station in the city or in a close neighborhood. A Y-Y transformer steps down the voltage to 1.5 kV which is the voltage at which the loads (distribution network on consumers' side in the micro grid) operate. The loads in Figure 4.1 represent the residential and commercial customers whereas all the thermal storage devices, including residential and commercial are modeled as a lumped thermal storage in the simulation. Moreover, the renewable sources in Figure 4.1 simulate the distributed renewable sources in the micro grid. The renewable energy sources are modeled as the current source with resistance in parallel and they provide powers at constant phase angle.

Although it is conventional to ignore the stator dynamics in transient simulations; that is, using synchronous generator one-axis or two-axis models, here we simulate the generator using a more detailed model including stators dynamics. However, the controller employs the generator one-axis model, as proposed in (3.37) to provide the storage control signal.

The MATLAB/Simulink model developed for this thesis is shown in Figure 4.1.

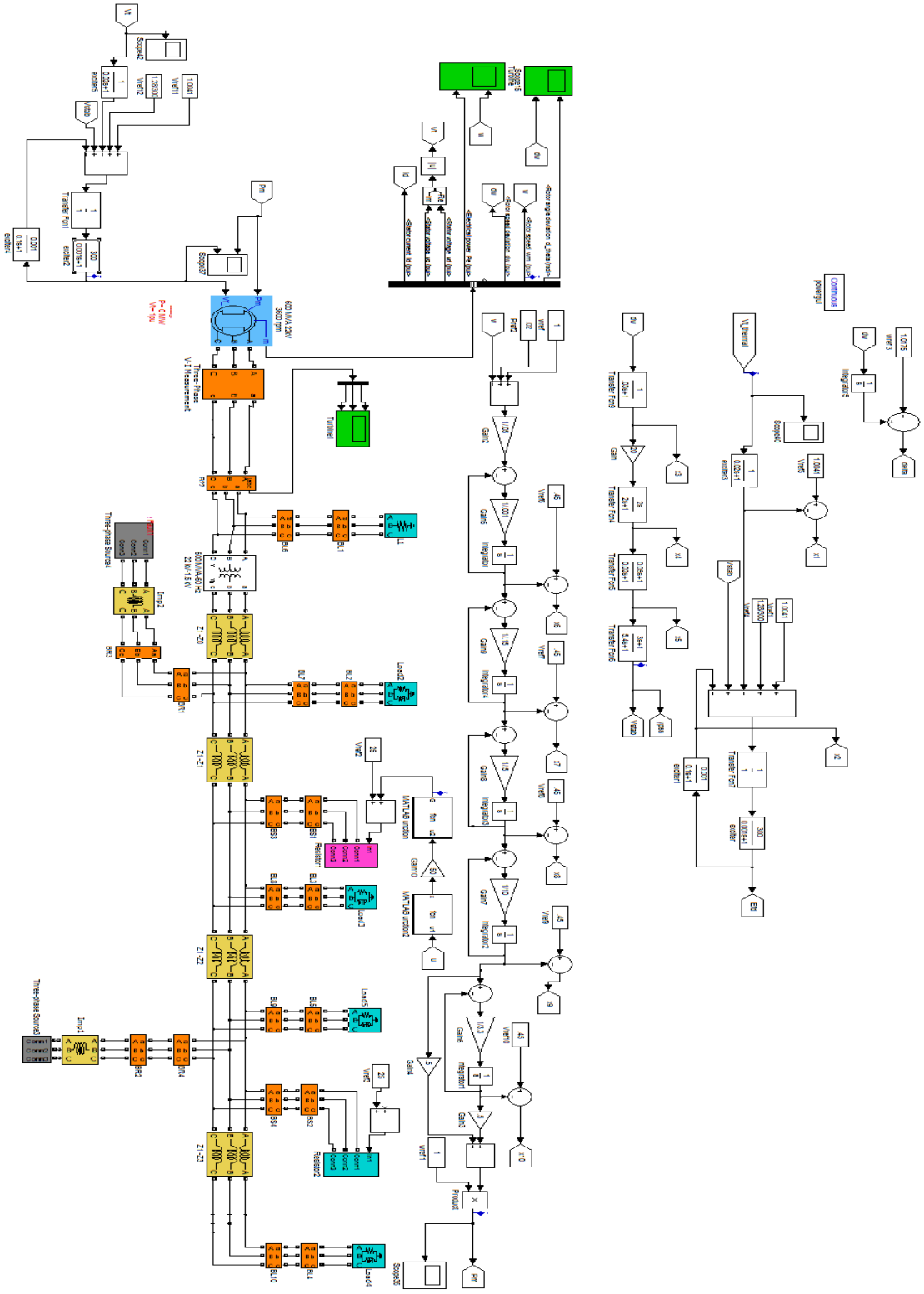

Figure 4.1 Simulink model of a micro grid designed in Simulink

The simulations are performed with resistive-inductive loads in the system. Reactive loads are more practical type of loads in the system with considerable number of induction motors used in residential and commercial appliances. The loads used in the simulation have a power factor of 85%. The simulation results are studied to observe the improvement in the behavior of the power system dynamics due to resistor type thermal storage over the power system stabilizer and governor (PSS+governor) after a fault, after a sudden load change in the system, and during unpredictable changes of renewable sources' generation. Also, each result is compared with the outcome obtained using a battery storage in the system instead of the thermal storage using the same optimal controller to control the power of the battery. In order to simulate the battery, a similar model to the thermal storage is utilized as the used model will eventually alter the power of the storage; however, the rate of absorbed power is restricted in battery storage as batteries possess lower absorbed power rates than the thermal storage. According to Table 1.1 it is shown that absorbed power rates are higher in thermal storage than batteries by a factor of 40% whereas these devices show the same power when giving power back to the system (injection power.) The injection power of the thermal storage can be interpreted as the portion of rated capacity that can be withdrawn from storage. In our simulations in case of thermal storage and battery, the original power system stabilizer and governor are retained. The optimal controller with both thermal and battery storage employs $R=0.65$ and $Q=diag\ (1, 1, 100, 1 \ldots 1)$ for the LQR controller to increase the frequency damping effect.

In all simulations, the thermal storage has an initial (steady-state) power, which is equal to the thermal power delivered to the buildings, and thus, no energy is stored in or extracted from the storage. During the disturbances, the power is different from the steady state and energy is stored or extracted from the thermal storage, and thus, the stored energy level is changed.

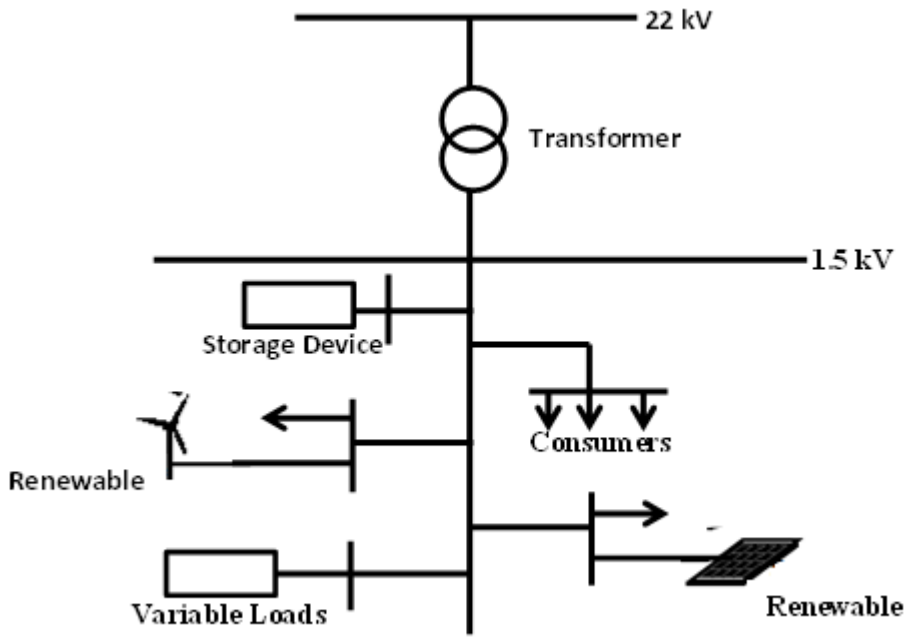


Figure 4.2 Micro grid structure of example 1.

### 4.1.1. Three-phase Fault

In this part, first, the frequency oscillations in the micro grid right after a fault is investigated with and without using thermal storage. For this purpose a three-phase fault is introduced close to the generator at $t = 8s$ and cleared at $t = 8.2s$. Figure 4.3(a) compares the damping effects of the PSS and governor with and without the thermal storage or battery, which shows that damping behavior is improved by operating the thermal storage. The absorbed/delivered power by the storage before and after the fault (steady-state) as well as during the fault (transients) is depicted in Figure 4.3(b).

Comparison of the performances of the thermal storage with the battery in Figure 4.3(a) demonstrates that although the battery can stabilize the system, the thermal storage still works better, which is due to higher absorbed power of thermal storage. According to Table 1.1, the charging (absorption) power of the battery is normally 40% of absorption power of the thermal storage with the same capacity; however, their discharge (injection) powers are the same.

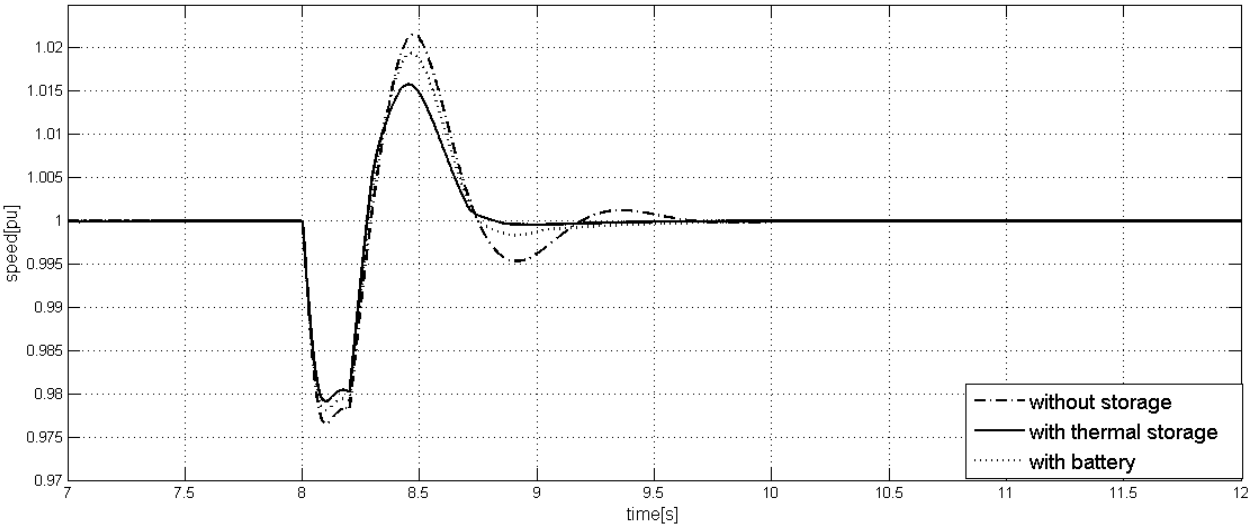


(a)

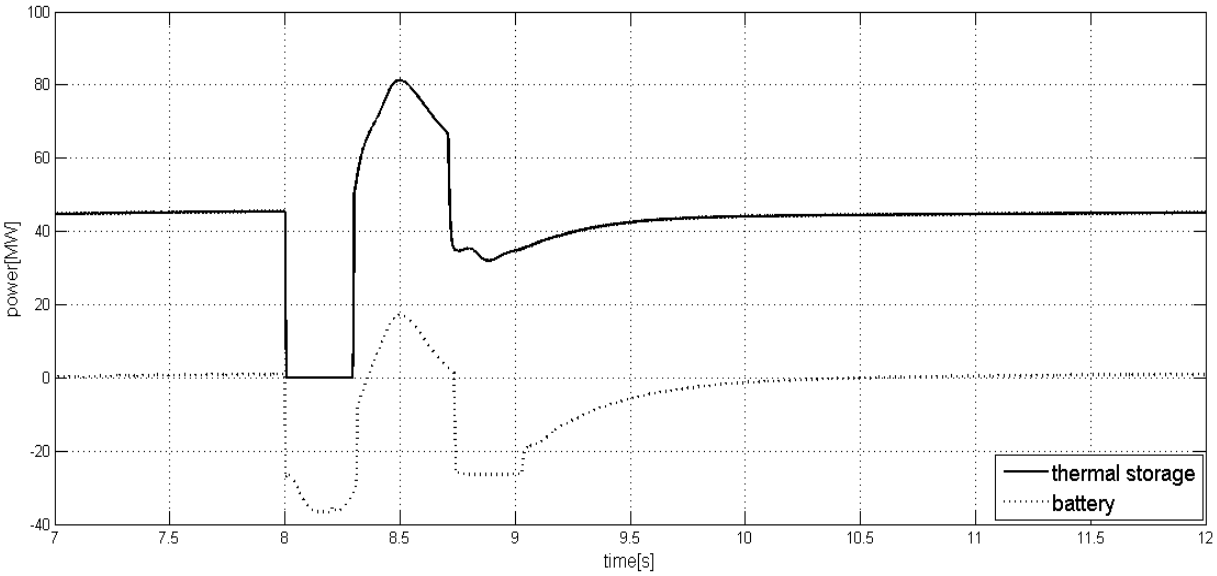


(b)

Figure 4.3 (a) Frequency oscillations of the micro grid under disturbance with no storage, with thermal storage, and with battery; (b) Active power absorbed by the thermal storages and battery (negative absorbed power in battery shows an injection or discharge of power to the micro grid)

In the simulation, hard limits are set on the battery power, accordingly, to limit its absorption power. Here the maximum discharge power level of the battery is set equal to the thermal storage maximum absorption power (about 40MW.) Moreover, since battery has no steady-state power consumption, the battery power stays at zero during steady-state operation.

### 4.1.2. Sudden Load Change

Next, the effect of a sudden change in the load is investigated in the micro grid. Figure 4.4 shows the case when total load in the system suddenly decreases by 20% at $t = 8s$. The thermal storage offers a rapid power compensation to improve the dynamic stability of the micro grid while the absored power of battery tends to exceed its maximum as seen in Figure 4.4(b). Also, as seen in Figure 4.4, the designed controller is robust and works even when the 20% load change in the system.

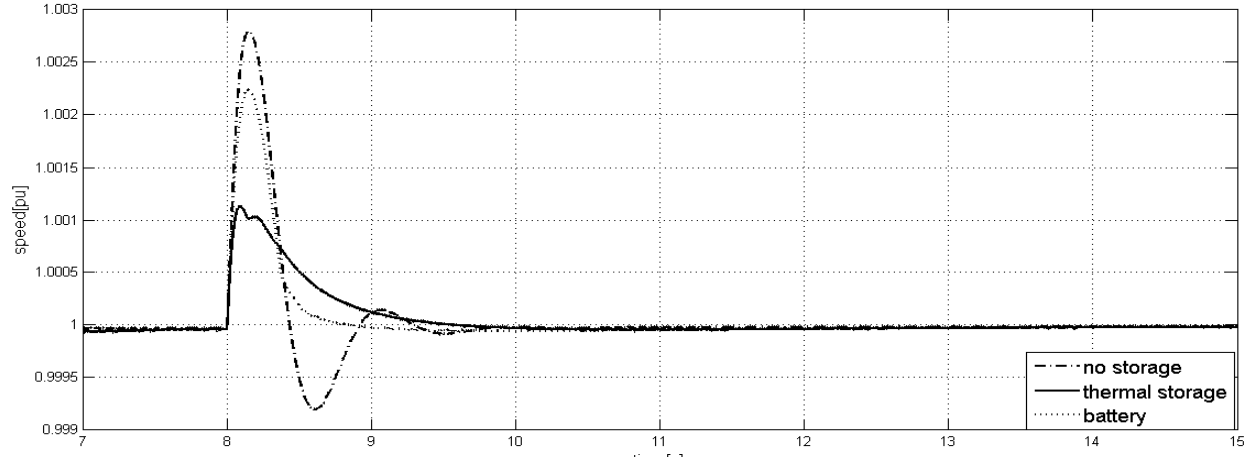


(a)

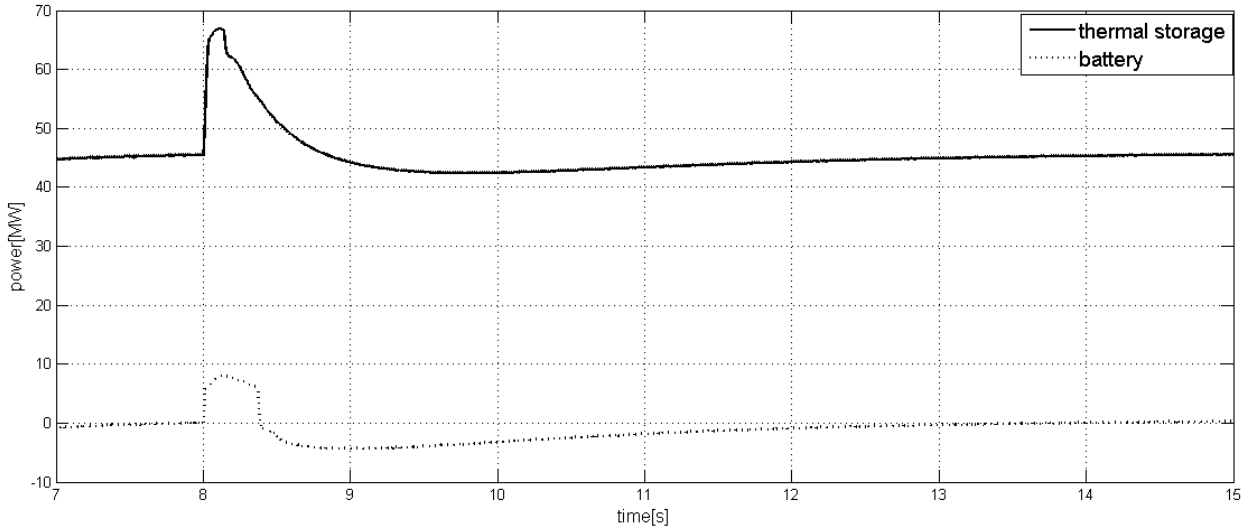


(b)

Figure 4.4 (a) Frequency oscillations of the micro grid under 20% load change in the load with no storage, with thermal storage, and with battery; (b) Active power absorbed by the thermal storage and battery

### 4.1.3. Renewable Energy Fluctuations

Finally, the effect of sporadic nature of renewable sources in the micro grid is investigated and the demand response through power adjustment in the storage is observed. This section is further divided into two parts to examine the fluctuations due to renewables appropriately.

#### 4.1.3.1. Change in the Renewable Source Power

Here, the total generated power of the renewables is subject to change as shown in Figure 4.5 as a result of a change in the ambient energy. For instance, when a solar source is present, clouds in the sky will decreace the power generated by the solar energy source. Similarly, a wind source produces less power when the speed of the wind decreases. After introducing the change in the renewable power source, the responses of the micro gird with and without storage are simulated.

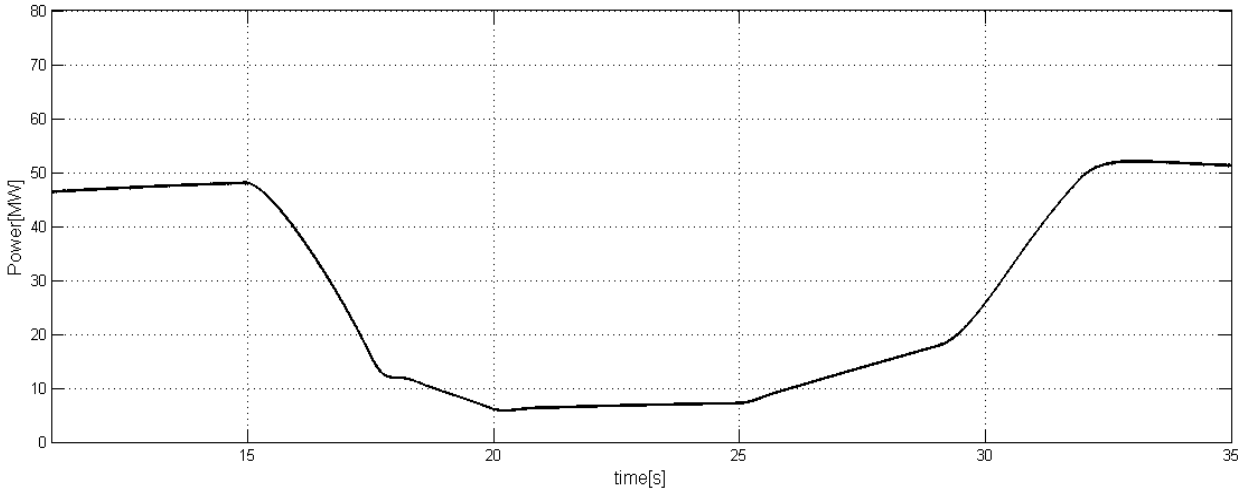


Figure 4.5 Change in the power generated by renewable sources

As shown in Figure 4.6(a), upon occurring the renewable power variations, frequency variation observed is not as significant with or without the battery and resistor type storage. However, as observed in Figure 4.6(b), in the case when only PSS and governor try to stabilize the system the voltage drop is substantial compared to the case when thermal storage or a battery is working with the grids.

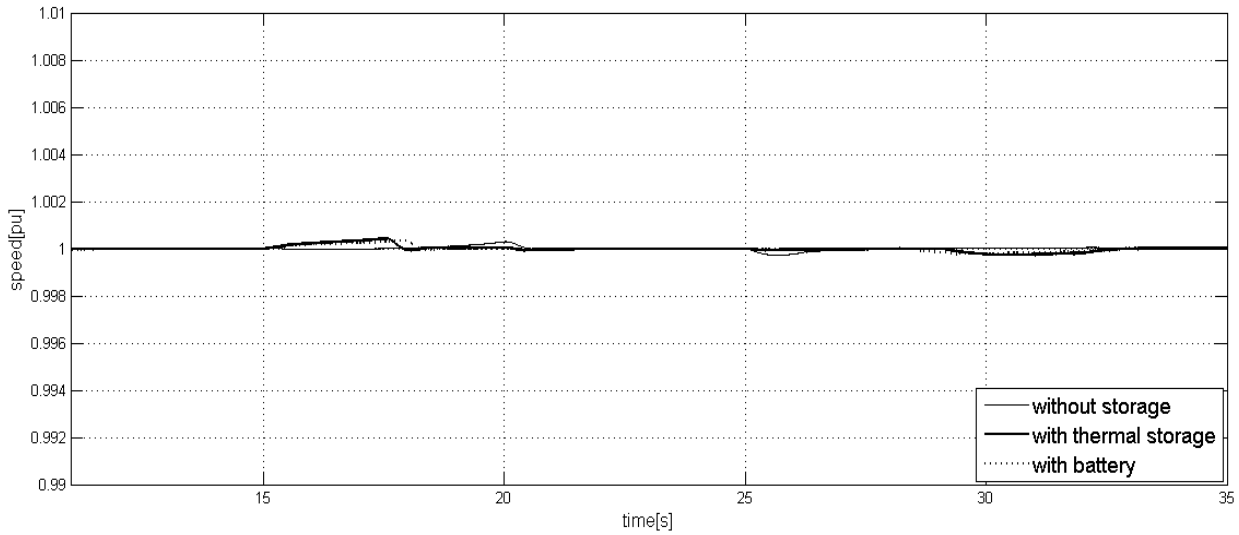


(a)

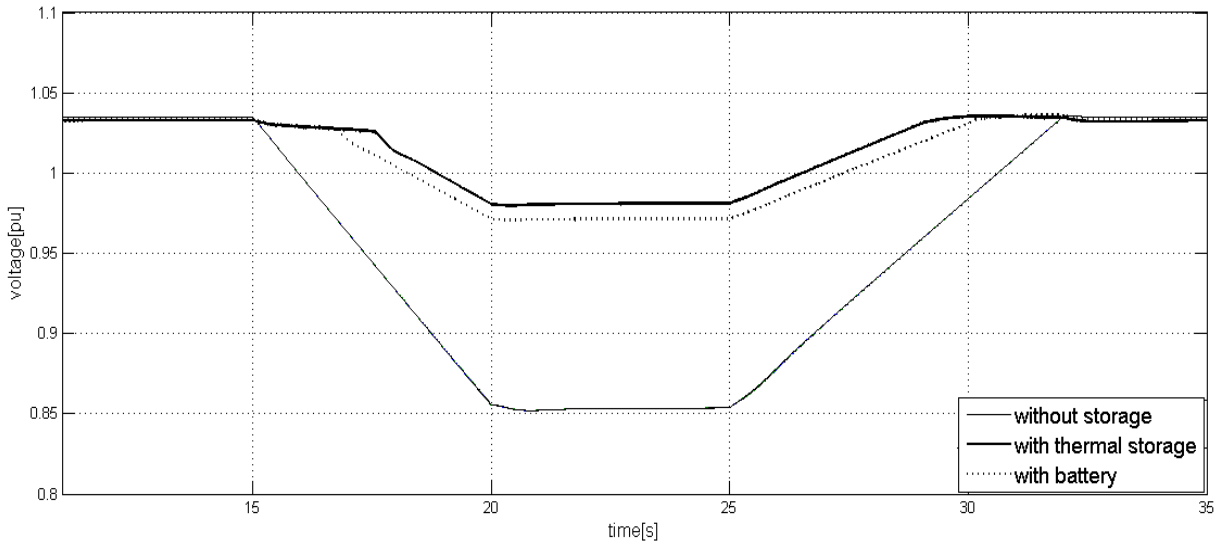


(b)

Figure 4.6 (a) Frequency oscillations of the micro grid caused by the intermittent renewable source with no storage, with resistor type thermal storage, and with battery; (b) Voltage profile at a selected bus in the micro grid in the absence and presence of storage and battery

Hence, the power absorption by the thermal storage and the battery is rapidly adjusted to the changes of the ambient energy to mitigate the voltage drop in the micro grid caused by variable generation and to prevent power changes in the synchronous generator (demand response). Although

Figure 4.6(b) depicts the voltage of only a selected bus, a similar behavior was be seen in other buses as well.

As discussed earlier in chapter 2 above, heat pump thermal storage can adapt to the intermittent slow changes (in the range of a few seconds and longer) of the renewable sources' generated power. Thus, it is expected that voltage variations due to intermittent renewable sources are mitigated by heat pump thermal storage, which is displayed in the following Figure 4.7. Figure 4.7 compares the voltage profile at a selected bus with and without a heat pump and as indicated, the voltage drop has notably improved when a heat pump is used than the case when only PSS and governor are working to stabilize the system.

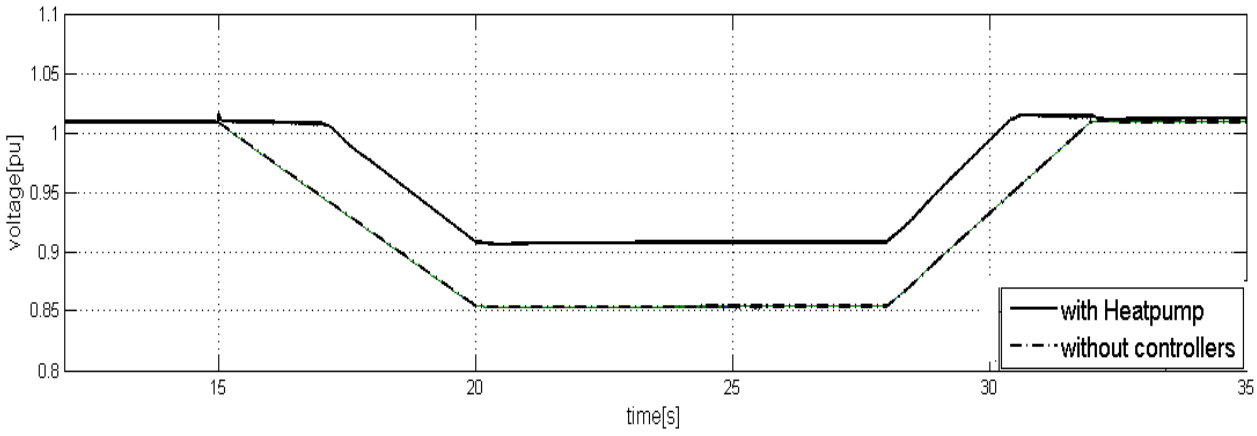


Figure 4.7 Voltage profile at a selected bus in the micro grid in the absence and presence of heat pump

### 4.1.3.2. Random Change in the Renewable Source Power

The change in the power generated by the renewable source is usually not as smooth as discussed in the section 4.1.3.1 above. The generation of power follow erratic path not easily recorded. Hence, to confirm that thermal storage is a better option in the micro grids in either case, one more simulation is performed assuming that the power produced by the renewable source is as random as shown in Figure 4.8. Thus, for the final part of the simulations in the first case, the renewable sources powers in the micro grid are subject to change as shown in Figure 4.8. The Figure shows the irregular power generated by the renewable sources in the system that can increase or decrease depending on the various factors.

As seen in Figure 4.6 above, the thermal storage and battery work in a similar manner to establish flatter trend in the grid. Hence, in this segment the result of battery is not shown.

Similar to the previous case, Figure 4.9(a) displays that no considerable frequency oscillation is observed in the system when only PSS and governor are working. However, as suggested in Figure 4.9(b) the voltage profile improves substantially when thermal storage is used in addition to PSS and governor.

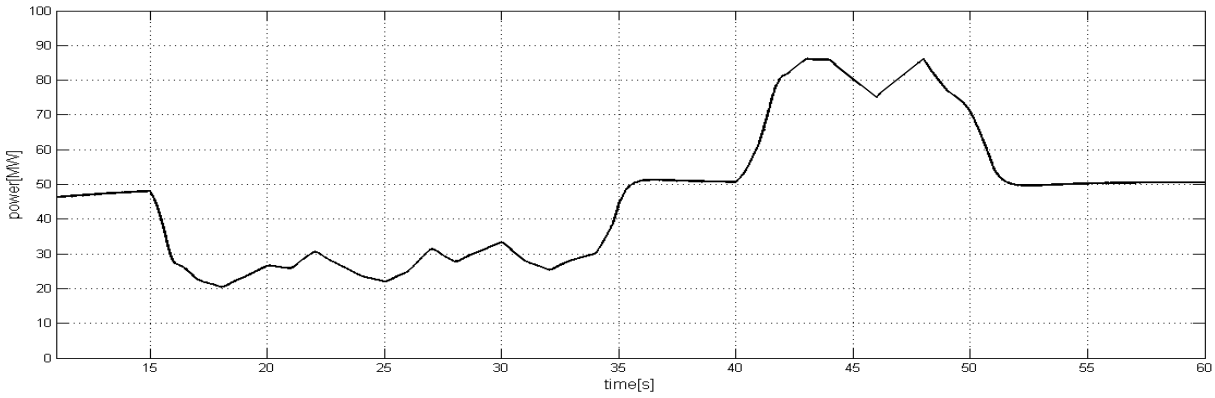


Figure 4.8. Intermittent changes in the power generated by renewable sources

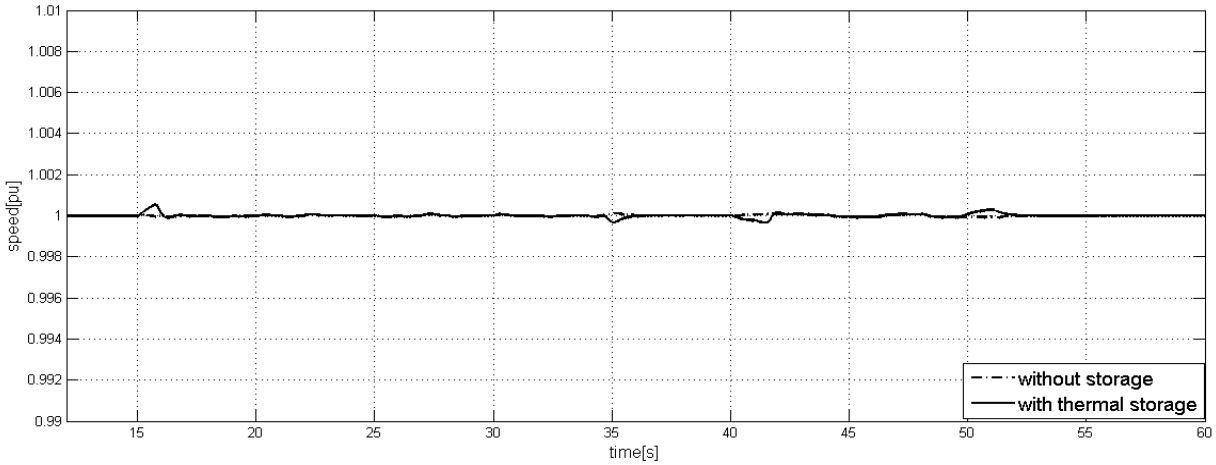


(a)

Figure 4.9 (a) Frequency oscillations of the micro grid caused by the intermittent renewable source with no storage and with resistor type thermal storage (b) Voltage profile at a selected bus in the micro grid in the absence and presence of thermal storage

(Figure cont'd)

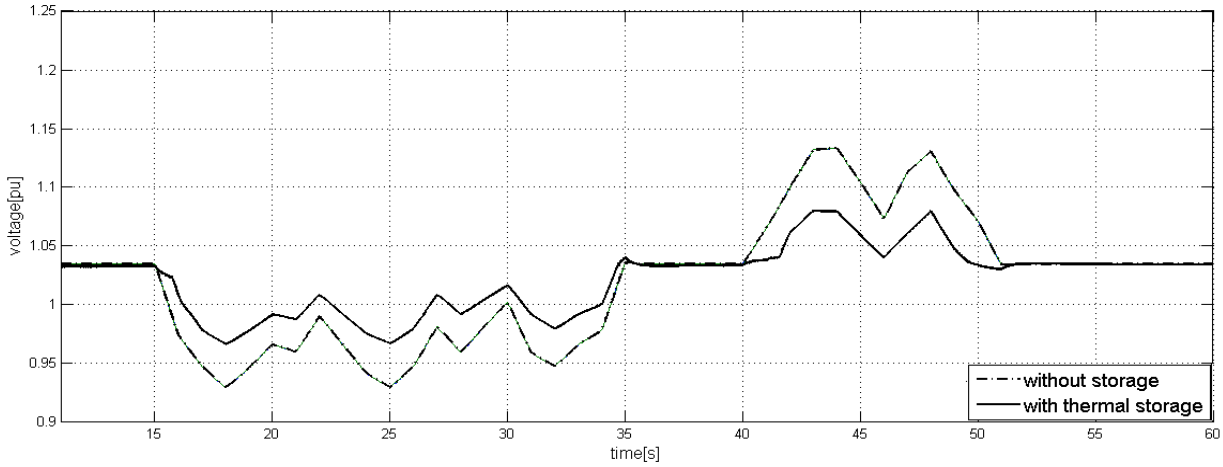


(b)

## 4.2. Simulation Example 2

Next, we perform our simulation and analysis on Design 2. The second topology is similar to the LSU micro grid system. The generator and the transformer parameters were obtained from the facility services at LSU. This system is initially built in ETAP to obtain the initial parameters in per unit. The model built in ETAP is shown in Figure 4.10. This LSU micro grid has a gas turbine of power 20 MW operating at 13.8 kV which is modeled as a synchronous generator with the parameters given in Table 4.1. The rest of the campus required power is provided from Entergy's main transmission grid modeled as an infinite bus in the ETAP system.

Table 4.1 Parameters of the synchronous generator in the second model

| Power | Power Factor | Voltage | Frequency | Xd | X'd | X"d | X2 | X0 |
|---|---|---|---|---|---|---|---|---|
| 20 MW | .85 | 13.8 kV | 60 Hz | 1.76 | 0.20 | 0.15 | .17 | 0.082 |

The main transmission grid has a high voltage of 69kV which is stepped down to 13.8 kV through Delta-Y transformers. The power is transmitted to different regions of LSU at 13.8 kV and is stepped

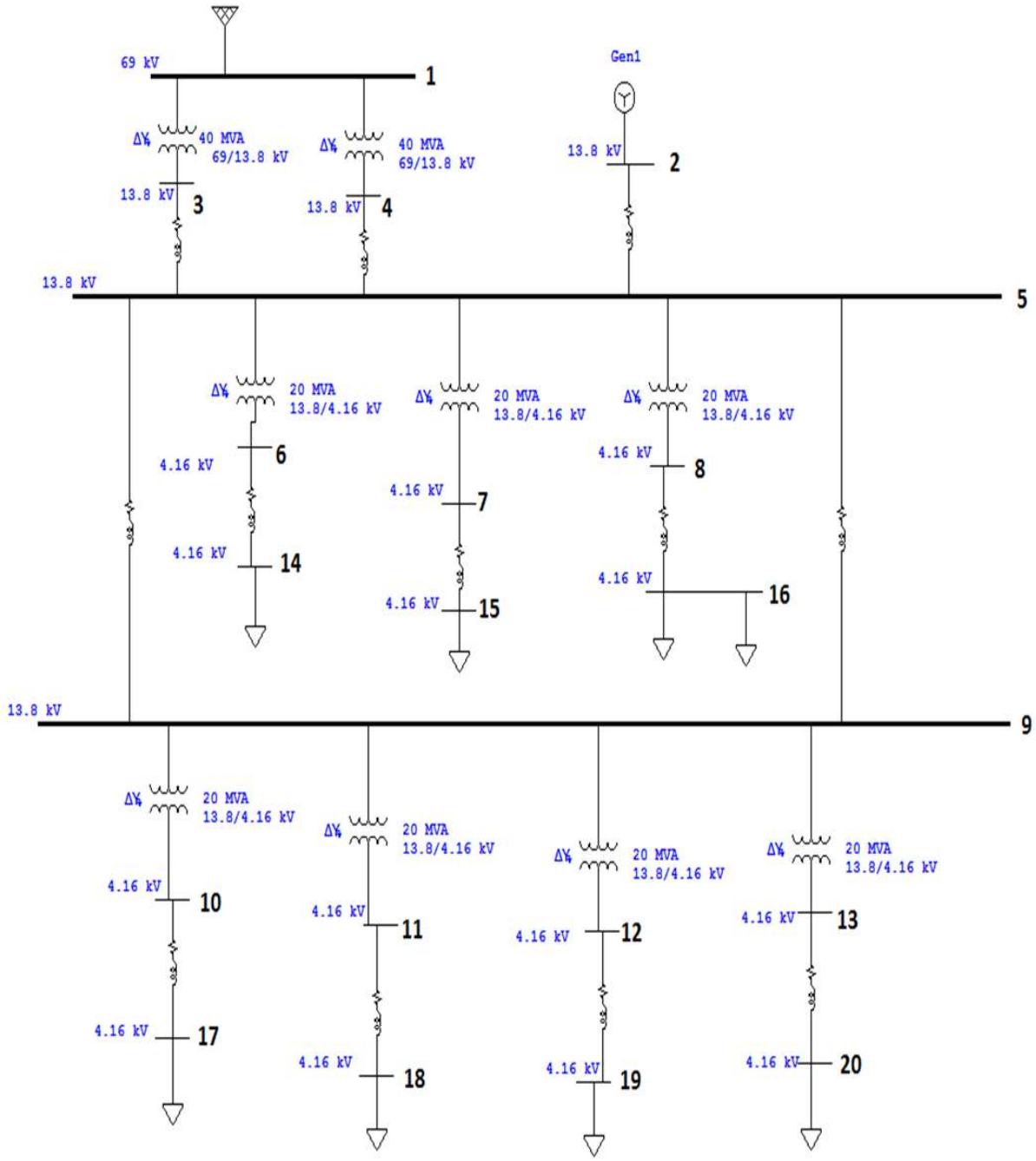


Figure 4.10 Model used for simulation of Design 2

down to 4.16 kV for operation. We assume that the lumped loads shown in Figure 4.10 are regions at LSU representing a group of buildings and offices at LSU. After obtaining the initial bus and line parameters from the ETAP model, load flow is obtained using MATLAB code. Compensators are added to the system to maintain the voltage profile of the system. The renewable sources are modeled in this

topology as constant power sources that can fluctuate. The states are produced directly (without observers) and fed through the controller to obtain our input for the system. In the ETAP model the system is connected to the main grid and the main grid is modeled as an infinite bus. Transient simulation is performed in MATLAB we follow similar approaches as discussed in sections above. We utilize LQR controller as a proper stabilizer in the system. In order to simulate the battery, a similar model to the thermal storage is utilized for the reasons discussed in section 4.1. The controllers employs R=100 and Q=diag (1, 100,1, 1, 1 … 1) to increase the frequency damping effect. Then, the following cases are simulated.

### 4.2.1. Three-Phase Fault

A fault is introduced in bus 2 near the synchronous generator at *t=15.5s* and cleared at *t=15.7s.* Then, the program gives the results first without the controller, the oscillations of the 20MW generators are recorded and then the controllers are introduced in the form of thermal storage and battery.

Figure 4.11(a) displays the deviation of the speed of the generator with respect to the center of inertia. As depicted in Figure 4.11(a), when only PSS is working as a stabilizer in the system, more deviation is present during the fault and also the damping of the oscillation takes longer. However, when the controllers are used speed deviation is less and for a shorter duration. Figure 4.11(b) demonstrates that as discussed in previous sections the charging (absorption) power of the battery is normally 40% of absorption power of the thermal storage with the same capacity. Here, the full capacity of the thermal storage is about 0.2 pu, and hence the battery has the absorption power of about 0.08pu. However, their discharge (injection) powers are the same. Figure 4.11(c) illustrates the speed of the generator, and from the figure we conclude that with controllers the system comes to a steady state faster and with less oscillation compared to that of only PSS. Also, a closer look at the voltage oscillation in Figure 4.11(d) infer that the performance of the generator is enhanced when controllers (both thermal and battery) are used with the PSS against the conventional way of using only PSS as a stabilizer.

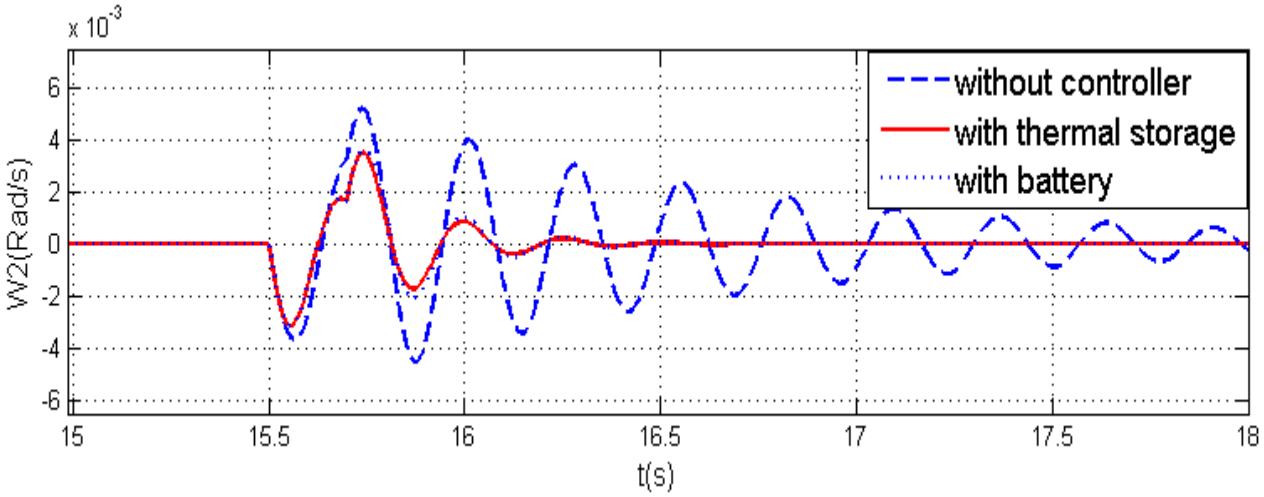


(a)

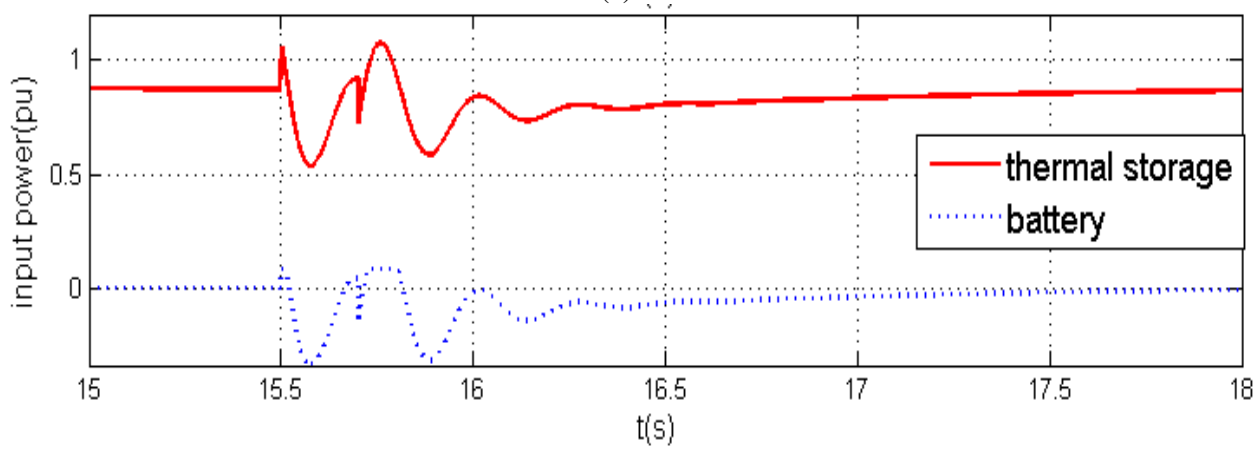


(b)

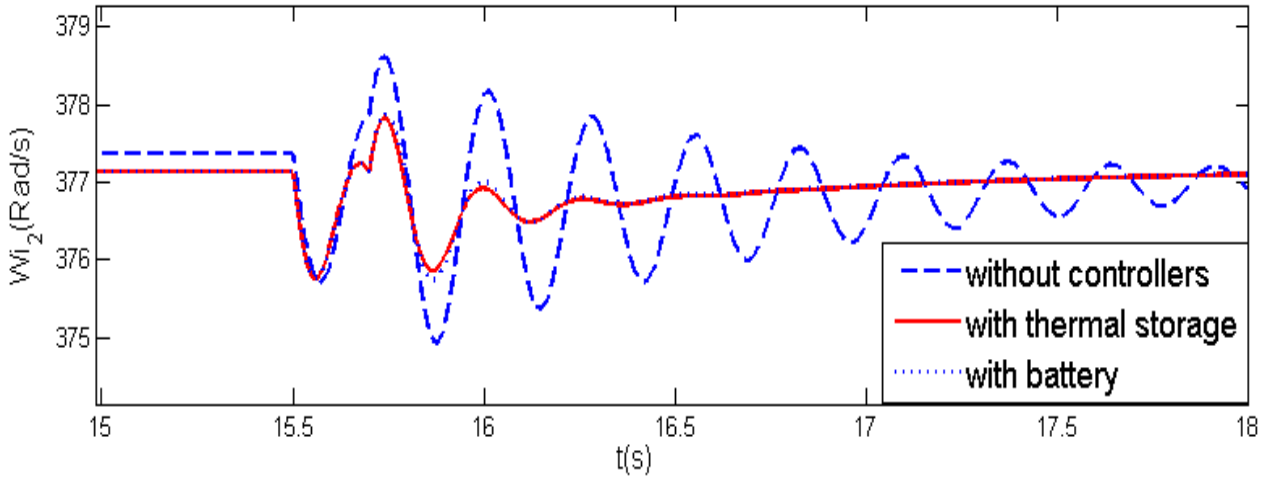


(c)

Figure 4.11 (a) Deviation of the speed of the generator with respect to the center of angular speed; (b) Active power absorbed by the thermal storage and battery; (c) Speed of the generator with and without the controllers; (d) Closer look at the voltage profile of a selected bus with and without the controllers.

(Figure cont'd)

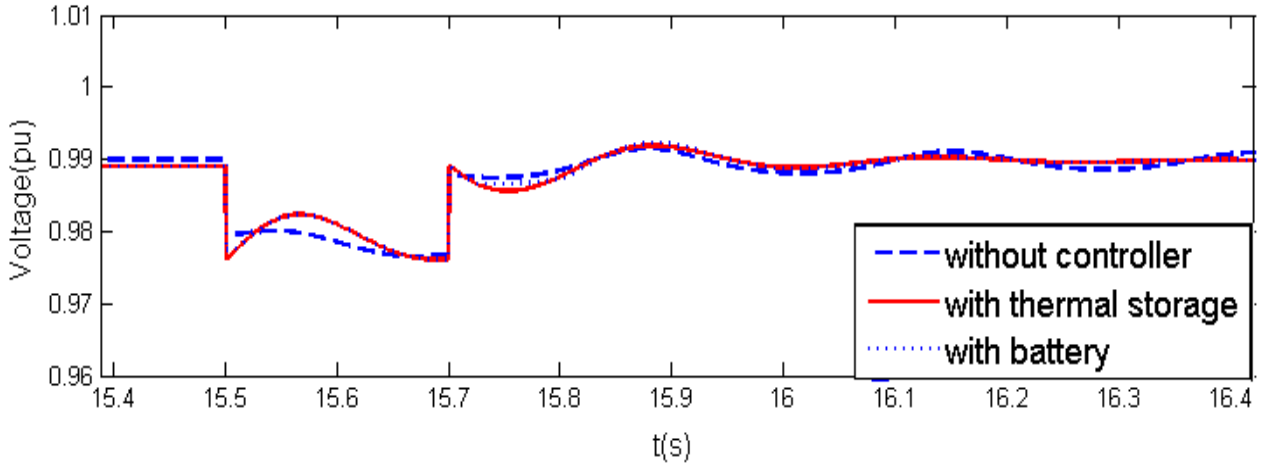


(d)

## 4.2.2. Sudden Change in the Load

For the second case study, the load of 0.8 pu is added in bus 2 when *t=12s* and removed when *t=13s* to create sudden load change. Figure 4.12 below depicts that a sudden change in the load causes fluctuation in the system. When the controllers are applied to the system the oscillation is considerably less. As indicated in Figure 4.12(c), the battery absorbs 40% of absorption power of the thermal storage with the same capacity. Figure 4.12 (b) illustrates the frequency of the generator in rad/s and Figure 4.12 (d) presents the voltage profile at a selected bus. In these figures we observe that the system performs better in damping the oscillations when batteries or thermal storages are present in addition to just the power system stabilizer.

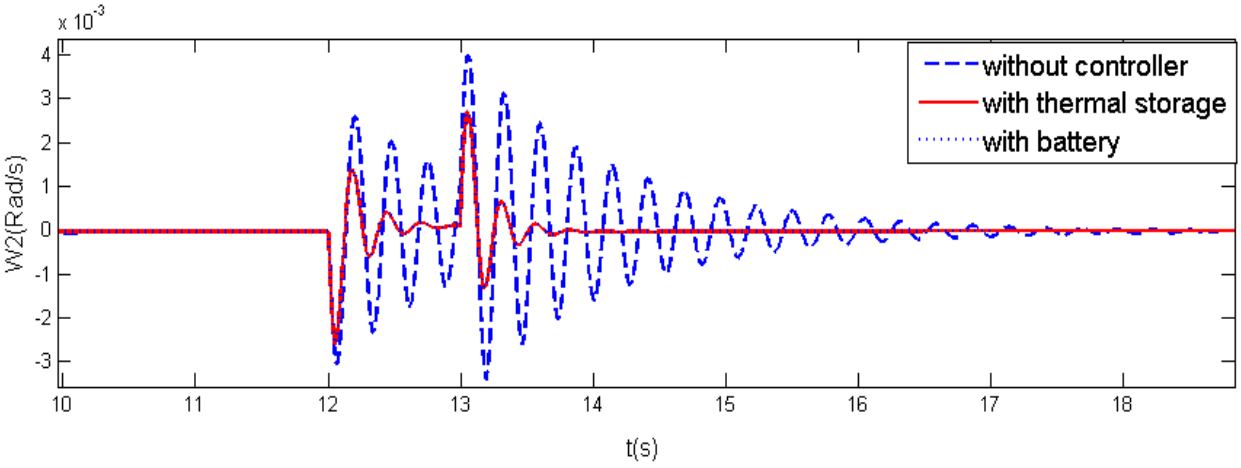


(a)

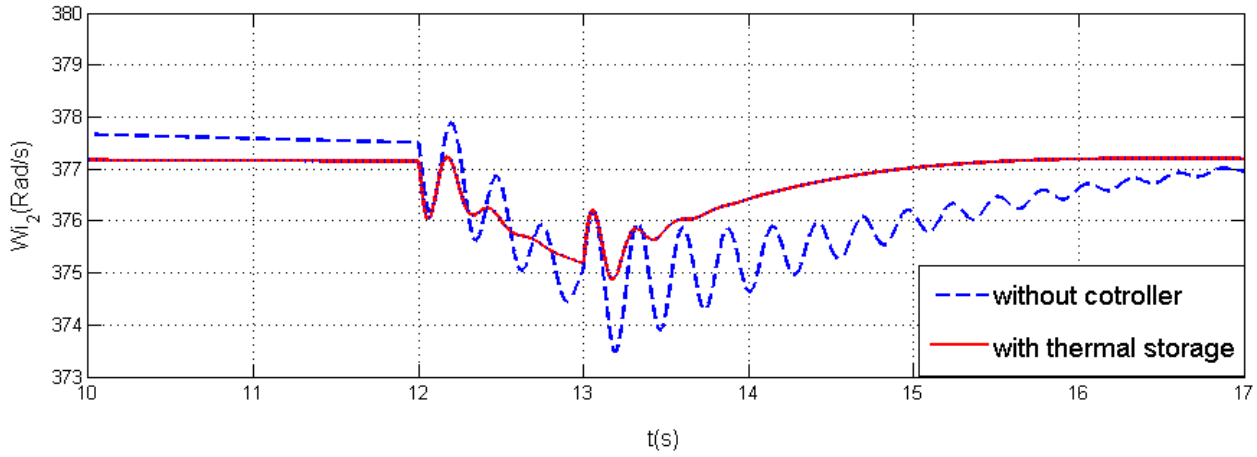


(b)

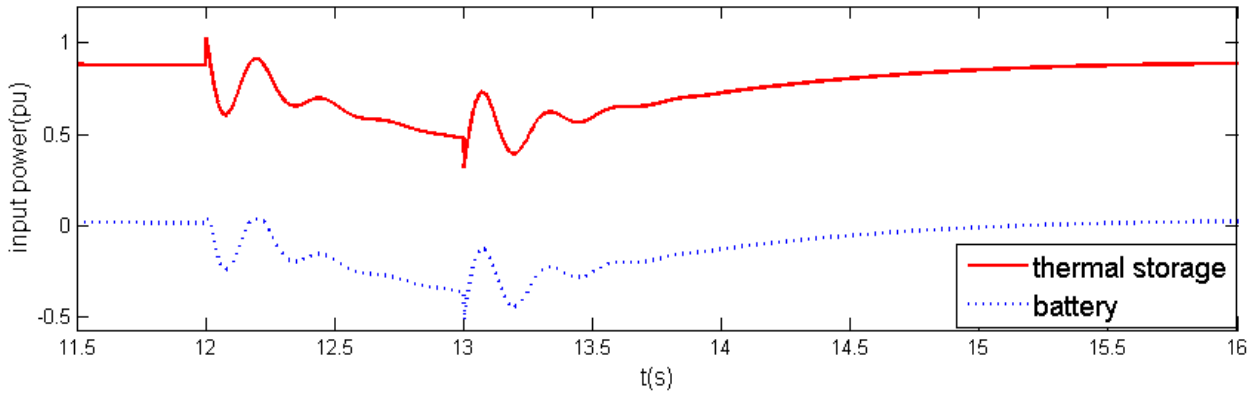


(c)

Figure 4.12 (a)Deviation of the speed of the generator with respect to the center of angular speed; (b) Speed of the generator with and without the controllers; (c) Active power absorbed by the thermal storage and battery; (d) Closer look at the voltage profile of a selected bus with and without the controllers.

(Figure cont'd)

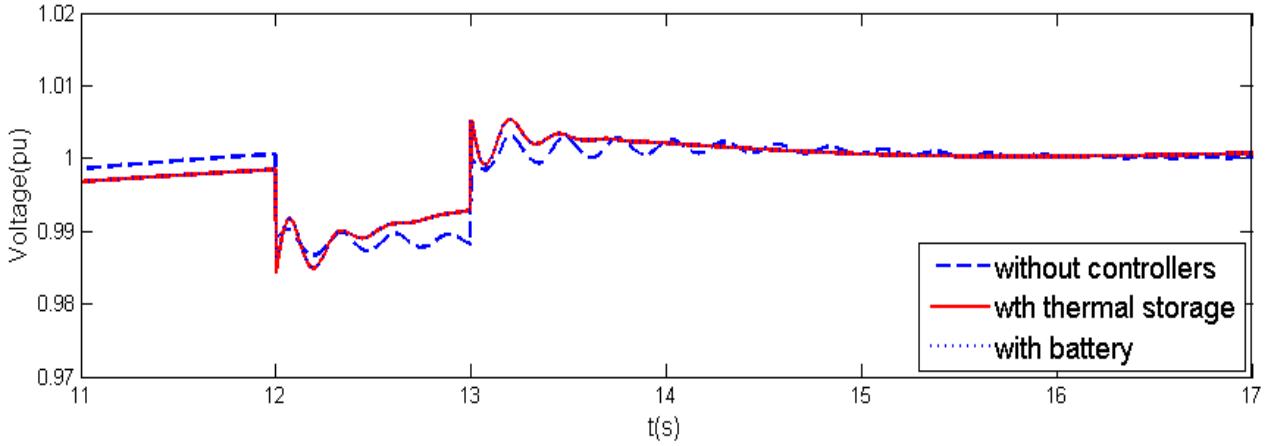


(d)

### 4.2.3. Change in the Renewables

As discussed earlier, the generation due to renewable is not constant for a variety of reasons. To test this system during such possible changes, a varying power generation is introduced in the model in the bus 2 again. Figure 4.13 illustrates the oscillation caused in the system due to the intermittent nature of the renewable energy source. The deviation of speed of the generator with respect to the center of the inertia is displayed in Figure 4.13(a). In this figure we distinguish that without the controllers the oscillation is more and the fluctuation fades away faster when controllers (battery or thermal storage) are in use.

Figure 4.13 (b) demonstrates the oscillation of the system due to the varying nature of renewables. As seen here, when thermal storage is used with PSS, the oscillation is much less compared to the case when only PSS and governor are used. Figure 4.13 (c) confirms that the absorption power of battery is 40% of absorption power of thermal storage.

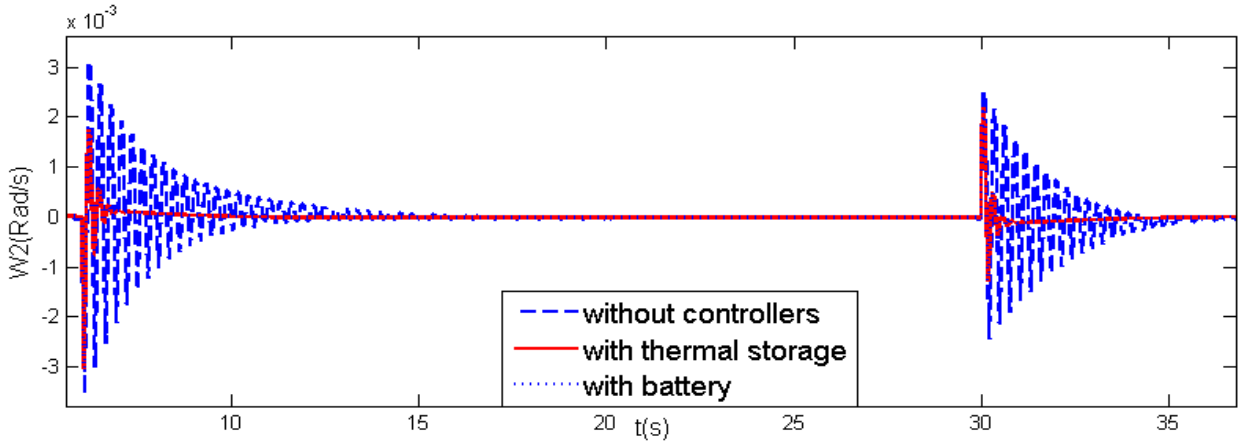


(a)

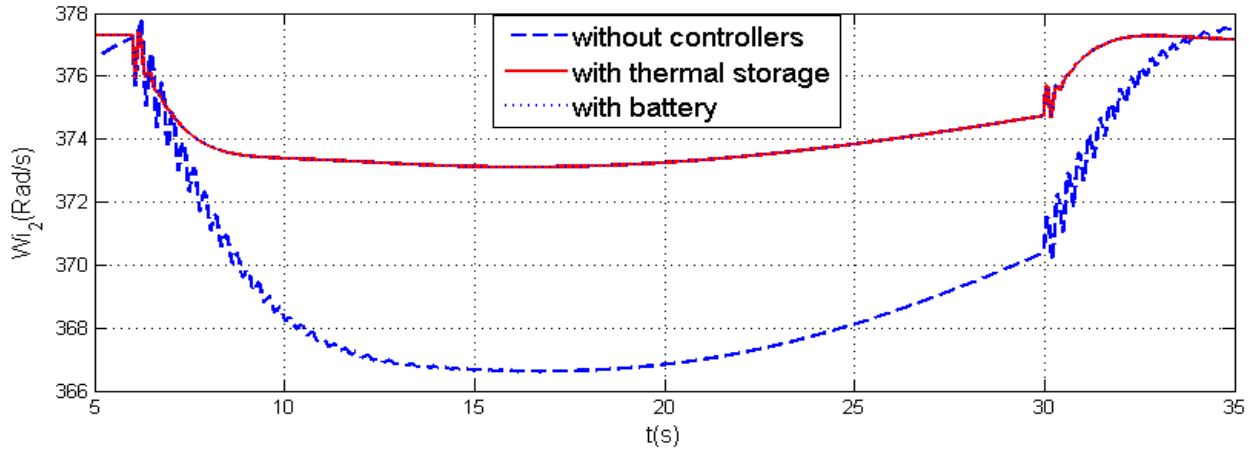


(b)

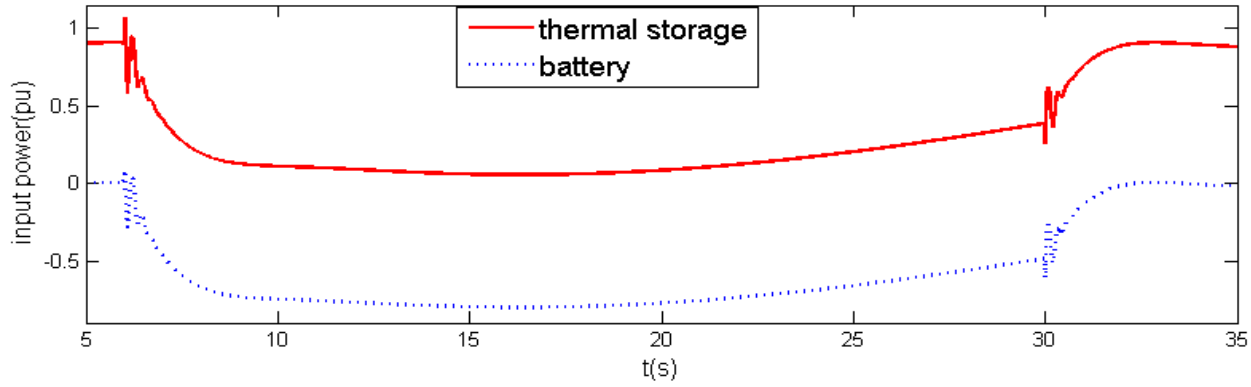


(c)

Figure 4.12 (a)Deviation of the speed of the generator with respect to the center of angular speed; (b) Speed of the generator with and without the controllers; (c) Active power absorbed by the thermal storage and battery; (d) Closer look at the voltage profile of a selected bus with and without the controllers.

(Figure cont'd)

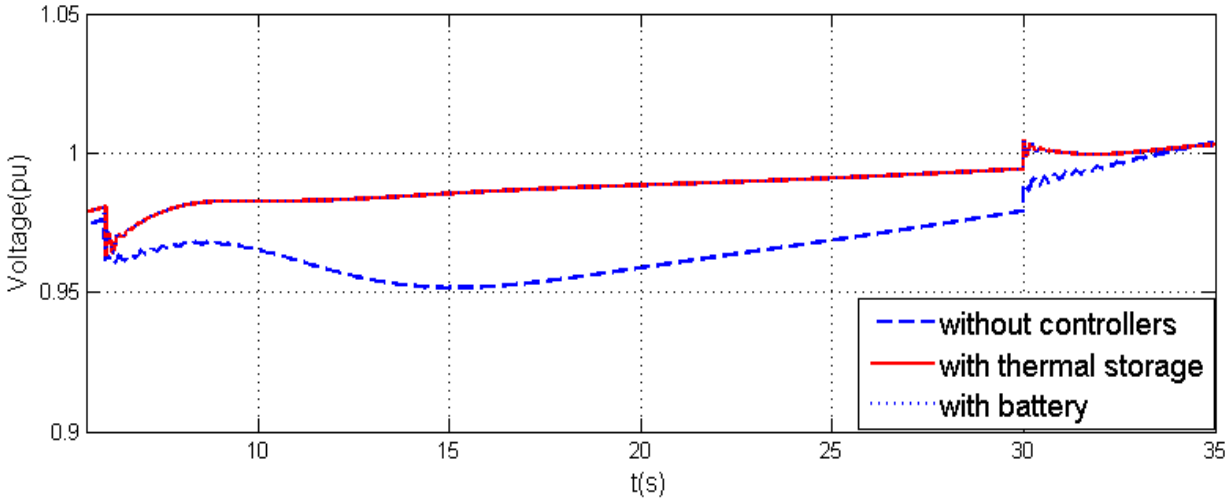


(d)

# CHAPTER 5
# CONCLUSION AND FUTURE POSSIBILITY OF STUDY

This chapter provides the conclusions to this thesis, offering a comparative study and analysis of the results obtained after a variety of simulations. A few of the possible avenues for further study on this topic are briefly discussed as well.

## 5.1. Conclusion

This thesis presents a model of a micro grid and employs the thermal, battery, and heat pump storage under various circumstances to improve the micro grid stability and demand response. Firstly, a power system with a synchronous generator, renewables, and storage is modeled with a set of differential and algebraic equation. Secondly, the equations are linearized to establish a linear system. Thirdly, an optimal LQR controller is designed using the dynamic states produced with and without the observers. Finally, the effectiveness of the controller to dampen the oscillation is examined for various case scenarios such as three-phase fault, sudden load change, and the sporadic nature of the renewables. The results obtained with the controllers are compared with the results attained with just the PSS and governor of the generator to dampen the disturbances. The proposed model and the simulations demonstrate that by using storage along with a proper controller in a micro gird the following can be achieved

1) Stability improvement attained over PSS and governor in fast transients such as faults
2) Voltage drop is significantly reduced during deviation in the renewable sources' power generations
3) Effective stabilizing mechanism and demand response obtained during sudden load changes in the power system, and
4) Thermal storage work better than a battery in achieving the goals due to its higher absorption power.

Hence, in the conclusion the effectiveness of the design and the approach is established as the results in chapter 4 demonstrate that storage can provide the instantaneous active power required to

enhance the dynamic stability of micro grid by varying the rate of absorbed power. Through mathematical evaluation and simulations, we observe that the storage provide better stability of the micro grids than conventional power system stabilizers alone.

## 5.2. Future Study

The analysis carried out in this thesis is based on a theoretical micro grid model developed in MATLAB/Simulink. The pragmatic and bigger topology is used to verify the theories established in the first model. There is only one thermal storage utilized in both the cases. The next stage, around which the future work should concentrate, is to analyze the performance and co-ordination of more than one controller. Similar approach as used in this thesis can be used to find the optimal controller.

# REFERENCES


[1] Robert H.Lasseter and Paolo Piagi, "Microgrid: a conceptual solution," *Power Electronics Specialists Conference, 2004. PESC 04. 2004 IEEE 35th Annual*, vol.6, no., pp.: 4285- 4290 Vol.6, 20-25 June 2004.

[2] C.L. Smallwood, "Distributed generation in autonomous and non-autonomous micro grids*," IEEE Rural Electric Power Conference*, 2002, pp.: D1 - D1_6, 2002.

[3] F. Katiraei, M.R. Iravani, and P.W. Lehn, "Micro-grid autonomous operation during and subsequent to islanding process," *IEEE Transactions on Power Delivery*, vol. 20, no. 1, pp.: 248 – 257, 2005.

[4] A. Molderink, V. Bakker, M.G.C. Bosman, J.L. Hurink, and G.J.M. Smit, "Management and control of domestic smart grid technology*," IEEE Transactions on Smart Grid*, vol. 1, no. 2, pp.: 109 – 119, 2010.

[5] G. Marshall, *Modeling of a micro grid system*, Bachelor Thesis, University of Newcastle, Australia. October 2004.

[6] A.M.L.L. da Silva, W.S. Sales, L.A. da Fonseca Manso, and R. Billinton, "Long-term probabilistic evaluation of operating reserve requirements with renewable sources," *IEEE Transactions on Power Systems*, vol.25, no.1, pp.: 106-116, Feb. 2010.

[7] K. Moslehi and R. Kumar, "A reliability perspective of the smart grid," *IEEE Transactions on Smart Grid*, vol.1, no.1, pp.: 57-64, June 2010.

[8] M. Stadler, "Distributed energy resources on-site optimization for commercial buildings with electric and thermal storage technologies," *Lawrence Berkeley National Laboratory*, June 2008.

[9] J. Marshall and M. Kazerani, "Design of an efficient fuel cell vehicle drivetrain, featuring a novel boost converter," *Proc. IEEE Ind. Electron.Conf.,* Raleigh, NC, Nov. 6–10, 2005.

[10] A. Burke, "Batteries and ultracapacitors for electric, hybrid, and fuel cell vehicles," *Proc. IEEE*, vol. 95, no. 4, pp.: 806–820, Apr. 2007.

[11] P. Mercier, R. Cherkaoui, and A. Oudalov, "Optimizing a battery energy storage system for frequency control application in an isolated power system," *IEEE Transactions on Power Systems*, vol.24, no.3, pp.: 1469-1477, Aug. 2009.

[12] A. Oudalov, D. Chartouni, and C. Ohler, "Optimizing a battery energy storage system for primary frequency control," *IEEE Transactions on Power Systems*, vol.22, no.3, pp.: 1259-1266, Aug. 2007.

[13] American Society of Heating, Refrigeration and Air-Conditioning Engineers, *Survey of Thermal Energy Storage Installations in the United States and Canada*, 1984.

[14] B. Arguello-Serrano and M. Velez-Reyes, "Nonlinear control of a heating, ventilating, and air conditioning system with thermal load estimation," *IEEE Transactions on Control Systems Technology*, vol.7, no.1, pp.: 56-63, Jan 1999.

[15] I. Dincer, "On thermal energy storage systems and applications in buildings," *Energy and Buildings*, vol. 34, no. 4, pp.: 377-388, May 2002.

[16] M. A. S. Masoum, P. S. Moses, and S. Deilami, "Load management in smart grids considering harmonic distortion and transformer derating," *Innovative Smart Grid Technologies (ISGT),* pp.: 1-7, 19-21 Jan. 2010.

[17] M. Stadler, "Distributed energy resources on-site optimization for commercial buildings with electric and thermal storage technologies," *Lawrence Berkeley National Laboratory*, June 2008.

[18] M. Anderson, M. Buehner, P. Young, D. Hittle, C. Anderson, Tu Jilin, and D. Hodgson, "MIMO robust control for hvac systems," *IEEE Transactions on Control Systems Technology,* vol.16, no.3, pp.: 475-483, May 2008.

[19] P. W. Sauer, and M. A. Pai, *Power System Dynamics and Stability*, Stipes, 2000.

[20] Ivan Jadric, *Modeling and control of a synchronous generator with electronic load,* Master Thesis, Virginia Polytechnic Institute and State University, January 1998.

[21] P. Kundur*, Power System Stability and Control,* McGraw-Hill, 1994, Section 12.5.

[22] Y. T. Wang, D. R. Wilson, and D. F. Neale, "Heat-pump control," *IEE Proceedings on Control Theory and Applications,* vol.130, no.6, pp.: 328-332, Nov. 1983.

[23] K. Ogata, *Modern Control Engineering,* Prentice Hall, 2002.

[24] S. J. Chapman, *Electric Machinery and Power System Fundamentals,* McGraw-Hill, 2002.

[25] K. Mekki, N.M. HadjSaid, D. Georges, R. Feuillet, "LMI versus non-linear techniques for the design of FACTS controller," *Power Engineering Society Winter Meeting, 2002. IEEE* , vol.2, no., pp.: 1501- 1505 vol.2, 2002.

[26] F. L. Lewis and V. L. Syrmos, *Optimal control*, New York, Weily, 1995.

[27] J.J. Grainger and W.D. Stevenson Jr., *Power System Analysis,* Tata McGraw- Hill, 2010.

[28] J. P. Hespanah, "LQG/LQR controller design, " *Undergraduate Lecture Notes,* April 1, 2007.

[29] E. Mouni, S. Tnani, and G. Champenois, "Comparative study of three modelling methods of synchronous generator," *IEEE Industrial Electronics, IECON 2006 - 32nd Annual Conference on* , vol., no., pp.: 1551-1556, 6-10 Nov. 2006.

[30] P. C. Krause, Analysis of Electric Machinery, New York: McGraw Hill, Inc., 1987.

[31] “Heat Pump Water Heaters.” Energysavers. 9 Feb. 2011. U.S Department of Energy, 18 April 2012.

# VITA

Sumiti Lamichhane was born and raised in Kathmandu, Nepal. After completing her high school in Kathmandu, she came to the United States for further studies. She completed her Bachelor of Science in Electrical Engineering from Louisiana Tech University, Ruston, LA in 2009 with *magna cum laude*. She is now pursuing Master of Science in Electrical Engineering while working as a research assistant at Louisiana State University, Baton Rouge, LA.